J. Micropalaeontology, 44, 213–235, 2025
https://doi.org/10.5194/jm-44-213-2025

Journal of Micropalaeontology
Open Access

Morphology of *Pulleniatina* (planktonic foraminifera) from optical microscopy, micro-CT, and SEM investigations

Alessio Fabbrini[1,2,★], Paul N. Pearson[1,★], Anieke Brombacher[3,4], Francesco Iacoviello[5], Thomas H. G. Ezard[3], and Bridget S. Wade[1]

[1]Department of Earth Sciences, University College London, Gower Street, London, WC1E 6BT, UK
[2]Department of Geography, University of Galway, Distillery Road 8, Galway, H91 CF50, Ireland
[3]Ocean and Earth Science, University of Southampton, National Oceanography Centre Southampton, European Way, Southampton, SO14 3ZH, UK
[4]Department of Earth and Planetary Sciences, Yale University, 210 Whitney Avenue, New Haven, CT 06511, USA
[5]Electrochemical Innovation Lab, Department of Chemical Engineering, University College London, Gower Street, London, WC1E 6BT, UK
★These authors contributed equally to this work.

Correspondence: Alessio Fabbrini (a.fabbrini@ucl.ac.uk)

Received: 12 December 2024 – Revised: 24 March 2025 – Accepted: 27 March 2025 – Published: 6 August 2025

Abstract. *Pulleniatina* is a genus of planktonic foraminifera that is widely used in biostratigraphic and palaeoceanographic studies. In our taxonomy, it comprises six morphospecies, alphabetically *P. finalis*, *P. obliquiloculata*, *P. praecursor*, *P. praespectabilis*, *P. primalis*, and *P. spectabilis*. Standard methods of taxonomic discrimination rely on descriptive characteristics of the adult test, such as the shape of the chambers, the shape and position of the primary aperture, the number of chambers per whorl, the height of the spire, the degree of involution, and the irregularity of coiling ("streptospirality"). Here, we illustrate representative specimens of each morphospecies and the likely ancestor, *Neogloboquadrina acostaensis*, from International Ocean Discovery Program (IODP) Site U1488 (Eauripik Rise, western equatorial Pacific Ocean) using light microscopy and X-ray microcomputed tomography (micro-CT). For each specimen, we provide multifocus light microscope images in three standard orientations, a set of up to 2000 X-radiographs, and a rendered three-dimensional (3D) model that can be viewed externally, internally, and in any cross-section using widely available freeware. We also include labelled images distinguishing each successive chamber and quantify the chamber volumes, the rate of size increase, the aspect ratios, and the angles at which they are added. A second set of specimens was crushed and imaged using scanning electron microscopy (SEM) to further study the internal morphology and wall texture. We use these observations to document the comparative ontogeny and test structure of the six *Pulleniatina* morphospecies in the context of an evolutionary model involving two diverging species lineages.

1 Introduction

The genus *Pulleniatina* is widely thought to consist of a single living biospecies, *P. obliquiloculata* (Hemleben et al., 1989; Schiebel and Hemleben, 2017; Brummer and Kučera, 2022; Morard et al., 2024), and several fossil morphospecies (Parker, 1965; Banner and Blow, 1967; Kennett and Srinivasan, 1983; Bolli et al., 1985; Pearson et al., 2023; Pearson et al., 2025). Its most characteristic feature is a dense, reflective, and non-porous cortex (CX; outer layer) that envelops most of the test. The genus evolved in the late Miocene about 6.50 ± 0.10 million years ago (Ma) in the form of *Pulleniatina primalis*, which seems to have evolved from the pre-existing species *Neogloboquadrina acostaensis* (Banner and Blow, 1967). Subsequent evolution can be divided into two lineages: one which produced a pinched, angulo-conical

morphology (*P. primalis* – *P. praespectabilis* – *P. spectabilis*) that became extinct in the Pliocene around 4.27 ± 0.05 Ma and another that produced a tendency for larger, more globular, involute, and irregularly coiled tests (*P. primalis* – *P. praecursor* – *P. obliquiloculata* – *P. finalis*) and survives today (Pearson et al., 2023). Discrimination between the various morphospecies is routinely achieved using optical microscopy of externally visible features, which, for practical purposes, must remain the case. However, the shape is sometimes difficult to interpret from the outside, chamber to chamber, especially because the more "advanced" members of the genus are often irregularly coiled and new chambers overlap and conceal pre-existing ones. Moreover, small, late-formed chambers can be difficult to detect below a smooth external surface.

A number of studies have attempted to better understand the internal morphology and affinities of *Pulleniatina*. As long ago as 1884, Brady (1884, Pl. 84, Fig. 20) illustrated a thin section of *P. obliquiloculata* that shows very clearly the thick wall and relatively simple morphology of the inner whorl. Parker (1965) illustrated a broken specimen of *P. spectabilis*, revealing the rounded chambers of the penultimate whorl which are similar to those of other pulleniatinids. Banner and Blow (1967) dissected several specimens of *P. finalis* and illustrated two specimens in thin section to reveal the inner juvenile morphology, which they found to have affinities with the supposed ancestor, *Neogloboquadrina acostaensis*. They also confirmed the highly irregular coiling mode. Postuma (1971) illustrated thin sections of *P. primalis*, *P. praecursor*, and *P. obliquiloculata*, confirming the close affinity of the three morphospecies and showing how successive chamber additions thicken the wall (discussed further below). Burt and Scott (1975) illustrated high-quality scanning electron microscopy (SEM) images of the inner whorl of broken *P. obliquiloculata*, showing a high, arched aperture on a rapidly expanding low trochospiral juvenile morphology that has five chambers per whorl. Subbotina et al. (1981) illustrated an acid-etched specimen of *P. obliquiloculata*, revealing the inner whorl as a low trochospiral with five chambers coiling around a distinctly different axis from the later chambers. Collectively, these contributions provide much useful information, but the images are necessarily static and two-dimensional (2D) and somewhat adventitious depending on the break or cut achieved.

More recently, several authors have illustrated dissected specimens in attempts to understand test construction and geochemistry. Kunioka et al. (2006) illustrated the wall structure using SEM and nanoscale secondary ion mass spectrometry (NanoSIMS) to produce Mg/Ca, Sr/Ca, and Ba/Ca distribution maps at micrometre resolution. Steinhardt et al. (2015) used a similar approach combined with laser-ablation ICP-MS analysis to profile Mg concentrations through the test wall of *P. obliquiloculata*. Both these studies found distinct compositional banding highlighted by high and low trace element concentrations. Lastam et al. (2023a, b) examined specimens of *P. obliquiloculata* which were acid-etched in epoxy resin, using backscatter and field emission SEM. They discovered differences in micro-texture in the different wall layers and areas of consistent crystallographic orientation. Chen et al. (2023) published X-ray microcomputed tomography (micro-CT) scans of several pulleniatinids from subsurface samples at ODP Hole 1115B, a drill core in the Pacific Ocean, making the raw data available online. Their data comprise several specimens each of *Pulleniatina praecursor*, *P. obliquiloculata*, and *P. finalis*, along with a variety of other species, although they did not discuss test morphology in detail.

Micro-CT is increasingly being used as a taxonomic aid in foraminiferal studies and to investigate patterns of shell growth and post-mortem dissolution (e.g. Görög et al., 2012; Iwasaki et al., 2019; Burke et al., 2020; Duan et al., 2021; Darling et al., 2023). The method produces very high resolution data that can allow construction of a three-dimensional (3D) mesh model from which individual chambers can be identified and shell parameters can be extracted (e.g. Burke et al., 2020; Brombacher et al., 2022; Darling et al., 2023). In this contribution, we use micro-CT scans to investigate the inner structure and ontogeny using representative specimens of fossil *Pulleniatina* species from a western Pacific drill site. A single representative specimen of each morphospecies was selected for characterization, except for *P. primalis*, where two specimens were used (a "primitive" form from soon after its first appearance and a later, more "advanced" form). The method is non-destructive, and the specimens are placed in a museum archive for posterity. A supplementary set of specimens was broken open and examined internally using SEM. We investigate these data to better understand the similarities and differences of the various morphospecies and their likely evolutionary relationships.

2 Methods

2.1 Study material

International Ocean Discovery Program (IODP) Site U1488 was drilled on the Eauripik Rise in the western equatorial Pacific (02°02.59′ N, 141°45.29′ E) in 2604 m water depth (Rosenthal et al., 2018). It is located in the waters of the Western Pacific Warm Pool, the hottest part of the open ocean, which is the core of the geographic range of *Pulleniatina* (Pearson et al., 2023). It was drilled using the Advanced Hydraulic Piston Corer in overlapping holes, providing stratigraphically continuous recovery. The dominant lithology is clay- and foraminifer-rich nannofossil ooze that forms a sedimentary deposit ∼ 310 m thick, dating back to ∼ 10 Ma in the Late Miocene. Age control is currently provided by nannofossil and planktonic foraminifer biostratigraphy and a series of palaeomagnetic reversals in the younger part of the succession (Rosenthal et al., 2018; Pearson et al., 2023), although it is likely that a more refined, astronomi-

cally tuned age model will become available in time. There are no hiatuses and no major sedimentary complications except for sea floor bioturbation. Planktonic foraminifer preservation is mostly very good, with minor dissolution and recrystallization (see Rosenthal et al., 2018, for a detailed assessment of the preservation state at various levels through the succession), and all *Pulleniatina* species are present in moderate to high abundance throughout the genus's evolutionary history. These factors make Site U1488 an excellent location for studying the evolution of *Pulleniatina*.

Sediment samples were washed over a 63 µm sieve. We selected representative adult specimens with the final-stage cortex for imaging, having studied the range of variation among populations at each sample level in the context of the morphology of the type specimens, the history of taxonomy in the genus, and the range of variation we have observed at other sites. Our collection initially included two specimens for each of the six *Pulleniatina* morphospecies and the putative ancestral species, *Neogloboquadrina acostaensis*; the best preserved and most representative from each pair was selected for detailed investigation after micro-CT imaging. However our final selection includes both specimens of *P. primalis*: one ("*P. primalis* 1") from near the beginning of the stratigraphic range, which has a partial external cortex and is a relatively "primitive" specimen, and a more typical morphology ("*P. primalis* 2") from ∼ 2 Myr later (Table 1). The biochronological positions of these study specimens are shown in Fig. 1 relative to the ranges and abundance fluctuations of the various morphospecies at the site. Each specimen was initially photographed in umbilical, spiral, and side views using a z-stacking light microscope and then scanned using micro-CT, from which a rendered 3D model was made. All except *P. primalis* 2 were then manually investigated to separate individual chambers, which were then analysed morphometrically, as described in the next subsection.

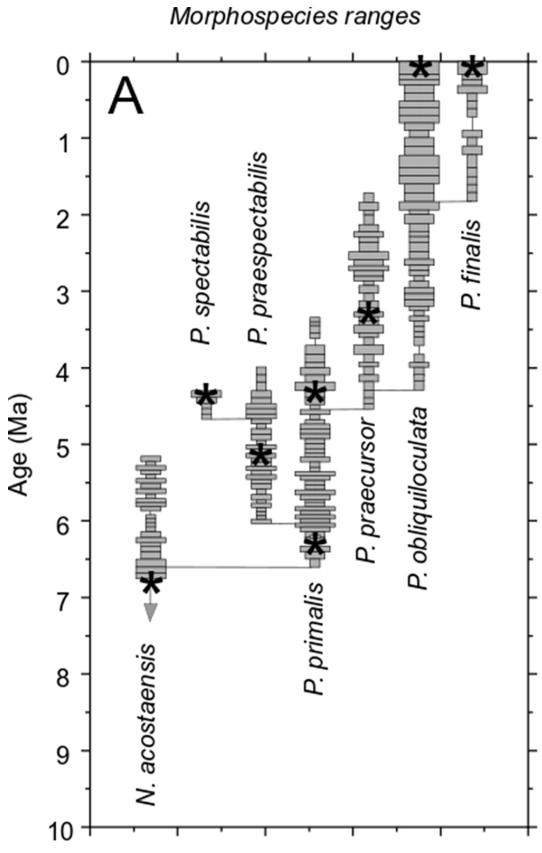

Figure 1. Geochronological ranges of *Neogloboquadrina acostaensis* and *Pulleniatina* species at IODP Site U1488. Bars on spindle plots represent qualitative abundance by visual estimation relative to the whole planktonic foraminifer assemblage, indicating, in order of decreasing width, "abundant" (> 20 % of the assemblage), "common" (> 10 %–20 %), "few" (> 5 %–10 %), and "rare" (< 5 %). Asterisks represent the ages of the individual specimens selected in this study. The older specimen of *P. primalis* is *P. primalis* 1, and the upper specimen is *P. primalis* 2. Modified from Pearson et al. (2023).

2.2 Optical microscopy

The study specimens were mounted successively in three standard orientations (umbilical, side, and spiral views) against a dark background and photographed with an Olympus automated multifocal z-stacking light microscope in the Department of Earth Sciences at University College London. For each view, up to 150 photographs were taken at different focal depths and were combined and sharpened to produce composite multifocus images using the software Stream Motion (Olympus).

2.3 Micro-CT

Micro-CT was conducted using the X-ray computed tomography microscope ZEISS Xradia 620 Versa, located at the Electrochemical Innovation Lab (EIL), part of the Department of Chemical Engineering at University College London. Specimens were mounted on a sample holder following the protocol described in Coletti et al. (2018). The sample holder was placed between the X-ray source and a 2 k × 2 k detector with a source-to-detector distance of 39.9 mm providing a voxel resolution of 500 nm using the 4X objective magnification in binning 1 mode. The instrument was operated at 120 kV and 14 W, employing a low-energy filter (LE4) to optimize transmission and the contrast-to-noise ratio. A total of 1601 radiographs were acquired over a 360° sample rotation range with an exposure time of 5 s per radiograph. For each specimen, the raw transmission images (.txrm) were reconstructed using a commercial image reconstruction software package (Zeiss XMReconstructor), which employs a filtered back-projection algorithm to generate the final reconstructed and corrected three-dimensional file. The final reconstructed files (.txm) were then exported as a stack of image files (.tiff) (hereafter, a "tiff stack") for further anal-

Table 1. The eight specimens that comprise this study, their provenance, and their reconstructed age. Specimens are deposited in the Natural History Museum, London (UK), as indicated by their "Museum ID".

Specimen number	Species	Museum ID	Sample level (363-U1488A-)	Age (Ma)
1	*N. acostaensis*	NHMUK PM PF 75513	22H-4, 79–81 cm	6.83
2	*P. primalis* 1	NHMUK PM PF 75514	20H-4, 81–83 cm	6.34
3	*P. primalis* 2	NHMUK PM PF 75515	12H-CC	4.34
4	*P. praespectabilis*	NHMUK PM PF 75516	16H-4, 80–82 cm	5.28
5	*P. spectabilis*	NHMUK PM PF 75517	12H-CC	4.34
6	*P. praecursor*	NHMUK PM PF 75518	9H-CC	3.29
7	*P. obliquiloculata*	NHMUK PM PF 75519	1H-2, 80–82 cm	0.01
8	*P. finalis*	NHMUK PM PF 75520	1H-2, 80–82 cm	0.01

ysis. A scrollable movie file was created to enable easy navigation through the tiff stack. The full set of images and movie files is available in Supplement.

2.4 Model construction and viewing

The reconstructed greyscale 3D image volumes (.txm files) were used to generate a three-dimensional surface made of a triangular mesh of voxels, using the Avizo 3D 2022.1 software package (Thermo Fisher Scientific). The 3D mesh files (.stl) can be viewed or manipulated in three dimensions using free software such as MeshLab (https://www.meshlab.net, last access: 24 June 2025). The models were further developed using the 3D-Tool Free Viewer (https://www.3d-tool.com, last access: 24 June 2025) software in which surfaces were colorized using default settings. The internal architecture of the models was investigated using the "Cross Section" tool, with the section outline shown as a red line. Screenshots of selected views were exported to make static figures, including standard external views: umbilical, side, and spiral. The 3D mesh files are available in the Supplement with instructions on how to manipulate and view the external and internal structure using MeshLab and 3D-Tool Free Viewer.

2.5 Chamber segmentation and analysis

The tiff stacks were imported into the free licence software OS Dragonfly. Chambers were manually segmented from the proloculus to the final chamber. The software permits visualization of three orthogonal views of the tiff stack. The "Active Contour" tool was used to interpolate between images, reducing the need for manual identification to about 1/10 of the original X-radiograph slices. The total number of slices examined depends on the size of the chamber being investigated; thus the earliest chambers, which are small, are composed of only 50–150 slices, whereas the final chambers are on average composed of 950–1000 slices. Adhering sediment on the inside surfaces of some of the specimens was easy to identify and was treated as void. Each chamber was segmented as a single region of interest (ROI), concluding with a final new object comprising all chambers merged in a single multi-ROI. The "Data Analysis" function on the multi-ROI was used to calculate the centroid xyz coordinates, voxel count, total volume (μm^3), surface area, and aspect ratio of each chamber. The data files (.csv) are available in the Supplement.

2.6 Growth trajectories

Growth trajectories in three dimensions were determined from the chamber centroid coordinates using the foram3D package (Brombacher et al., 2022) in the R environment for statistical and graphical computing (version 4.2.3; R Core Team 2020). The software determines the angle each chamber makes with its two predecessors ("chamber angle"), the angle each chamber makes with the plane defined by the three previous chamber centroids ("trochospiral angle"), the number of chambers in the final whorl at the time each chamber was built, the number of whorls, and the coiling direction of each chamber. The software also allows visualization and inter-comparison of the growth spirals in interactive three-dimensional plots, allowing the viewer to rotate the spirals freely in three dimensions and zoom in and out. This feature is particularly useful for understanding the geometry when it departs from regular trochospiral coiling (see below). The Supplement contains an annotated R script containing code to calculate all traits and to permit user visualization and manipulation.

2.7 Dissection

The specimens listed in Table 1 provided most of the data for our study in a non-destructive way, allowing them to be preserved in cardboard slides and deposited in a museum. A second set of specimens (one for each of the *Pulleniatina* morphospecies) was used for destructive investigation. These were mounted on steel pedestals using adhesive tape and photographed using the z-stacking light microscope. To avoid charging under the SEM, they were sputter-coated with gold in an argon atmosphere then imaged externally using the secondary electron detector in a JEOL JSM-6480LV microscope at the Department of Earth Sciences, University Col-

lege London. Specimens were then transferred to a second pedestal, where they were crushed under a glass slide. The resulting debris was sputter-coated for a second time and re-investigated at high SEM magnification.

3 Results

3.1 External morphology

Light microscope images of the selected specimens viewed in standard orientation are compared with screenshots of the rendered 3D models, aligned approximately in the same views (Fig. 2). The rendered models show features such as surface undulations, pustules, and sutures that may be less clear on the bland white surfaces. Together these images document the size, chamber shape, apertural morphology, and surface ornamentation of specimens that we consider typical of the various morphospecies, although, of course, every specimen has its own peculiarities.

3.2 Internal morphology and involution

The mesh models were manipulated in three dimensions and examined in various cross-sections to better understand the coiling geometry. Here we present two sets of cross-sectional cuts in approximately similar orientations on the various specimens to facilitate comparisons. The first set of cuts (Fig. 3a–h) was taken to reveal the proloculus and early whorl, which is difficult to see externally because the cortex tends to smooth out the sutures. In most cases, the early whorl lies close to the centre of the spiral side, although, in *P. finalis*, it is deeply buried in the test interior. These images help illustrate the relatively simple globular chambers of the initial whorl in all species but also highlight some differences between the specimens. The *P. finalis* specimen has a noticeably large proloculus, while that of *N. acostaensis* is very small. Most specimens have five chambers in the inner whorl, but *P. praespectabilis* and *P. spectabilis* have four (as described by Parker, 1965). The images also help determine the true number of chambers, which may not be obvious externally. For instance, following from its very small proloculus, *N. acostaensis* (Fig. 3a) has more chambers in the inner whorl than are obvious externally, totalling 18 chambers overall. What appears externally as a large enveloping final chamber in *P. finalis* in fact consists of three chambers of diminishing size with thick septa between them but virtually no indication of external sutures (Fig. 3h).

The second set of cuts (Fig. 3i–p) helps reveal the nature of the spire, which is overall relatively low in *N. acostaensis* and *P. spectabilis*, moderate in *P. praespectabilis*, high in *P. primalis* and *P. praecursor*, and very high in *P. obliquiloculata*. In *P. finalis*, the coiling pattern is less easy to visualize in any single cut, as is discussed further in Sect. 3.3 below. Particularly striking is the variation in thickness of the wall, which is very thin in *P. primalis* 2, notwithstanding its cortex, and extremely thick in *P. obliquiloculata* and *P. finalis*. The cross-sections also show how complicated the internal spaces become as the chambers overlap one another and their shapes becomes pinched or compressed, especially towards the end of the life cycle when chambers may also be relatively reduced in size.

The extent to which new chambers overlap and grow over preceding chambers is conventionally referred to as the degree of involution of a test. This aspect of the morphology is best explored using the 3D models. *Neogloboquadrina acostaensis* and *Pulleniatina primalis* 1 are moderately involute, with each new chamber typically encroaching slightly on its predecessor on the spiral (dorsal) side and extending to just short of the centre of the growth spiral on the ventral side, leaving a narrow but distinct central depression (umbilicus). *Pulleniatina primalis* 2, *P. praespectabilis* and *P. spectabilis* are all slightly more involute, especially on the ventral side, where chambers tend to lean over the umbilicus (as observed by Blow and Banner, 1967). Because of this, the umbilicus is often obscured or reduced to little more than a single voxel. Both *P. praecursor* and *P. obliquiloculata* are strongly involute on the ventral side such that the test no longer has a recognizable umbilicus. *Pulleniatina finalis* is strongly involute on both sides of the test, with the early whorls obscured and buried within the test, sometimes making it difficult to discern which side is which on external inspection.

3.3 Growth and development

The results of the chamber segmentation procedure are shown in Fig. 4. Note that the imaged chamber volumes are internal voids, so the walls between the chambers (septa) and the external test are omitted; hence these images are like virtual internal moulds. Because of this, *Pulleniatina obliquiloculata* and *P. finalis*, which have very thick walls, are much larger externally than they appear in this figure.

The growth spirals (lines that pass through the centroids of successive chambers) are best visualized using the interactive foram3D manipulation tool (Brombacher et al., 2022). Static screenshots are shown in Fig. 5, arranged looking down on the spiral (Fig. 5a–g) and orthogonally, showing the height of the spire (Fig. 5h–n). These images help illustrate significant differences in the coiling mode between the various morphospecies. Foraminifera are conventionally regarded as trochospirals (expanding helices), in which the height of the spire (trochospirality) is defined as the extent of translation along the vertical axis of the helix. This can differ between species and is frequently used as a descriptive and diagnostic character, as it is in other spiral organisms. It has long been recognized, however, that living pulleniatinids depart from a regular trochospiral arrangement during ontogeny. This was noticed as early as 1865, when *P. obliquiloculata* was first described (Parker and Jones, 1865), with the specific name referring to its oblique chamber arrangement. One way to visualize this irregularity is as a shift in the coiling axis itself,

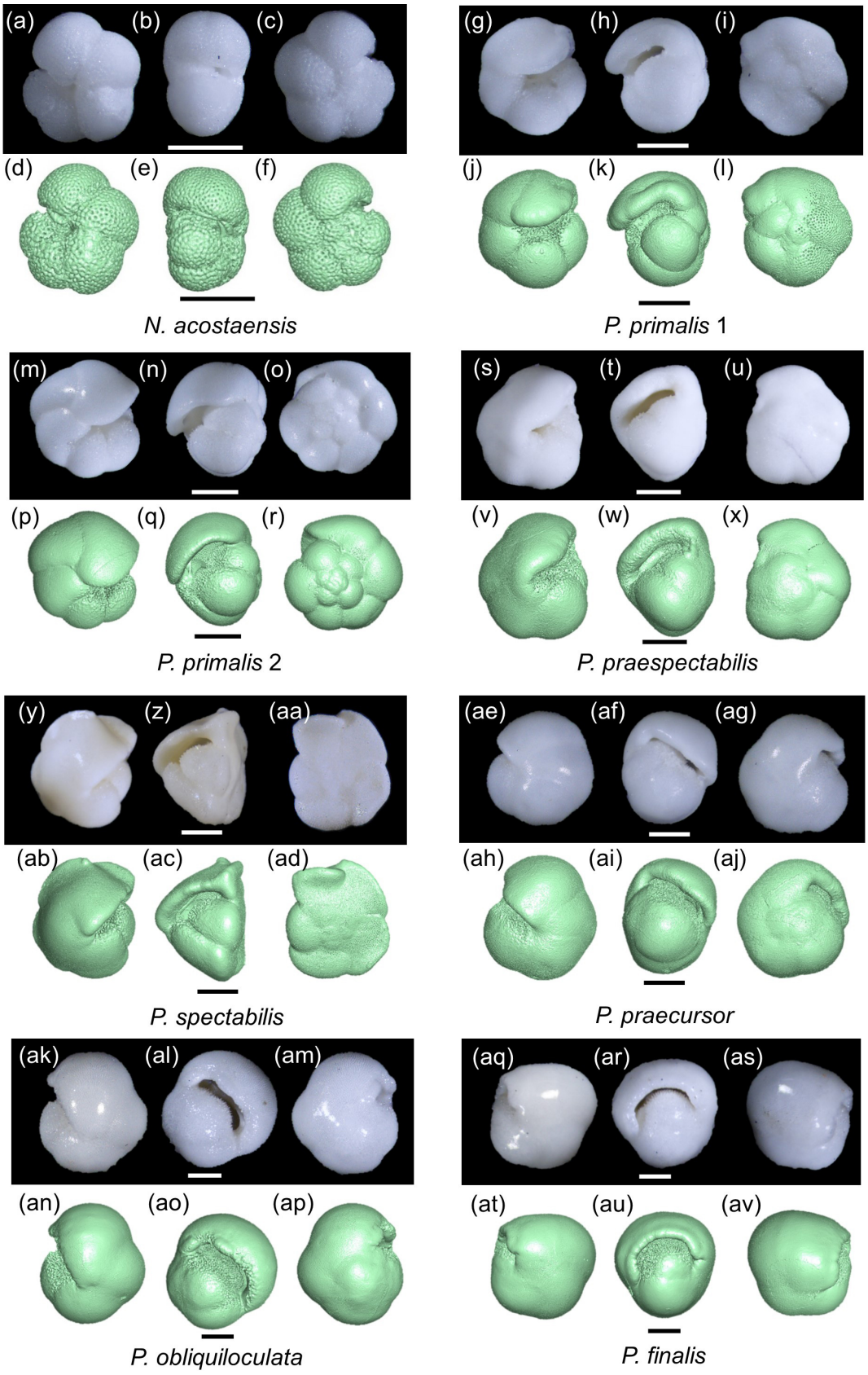

Figure 2. *Z*-stacked light microscope and micro-CT models of specimens 1–8 (Table 1) in umbilical, side, and spiral views. Scale bars are 200 µm.

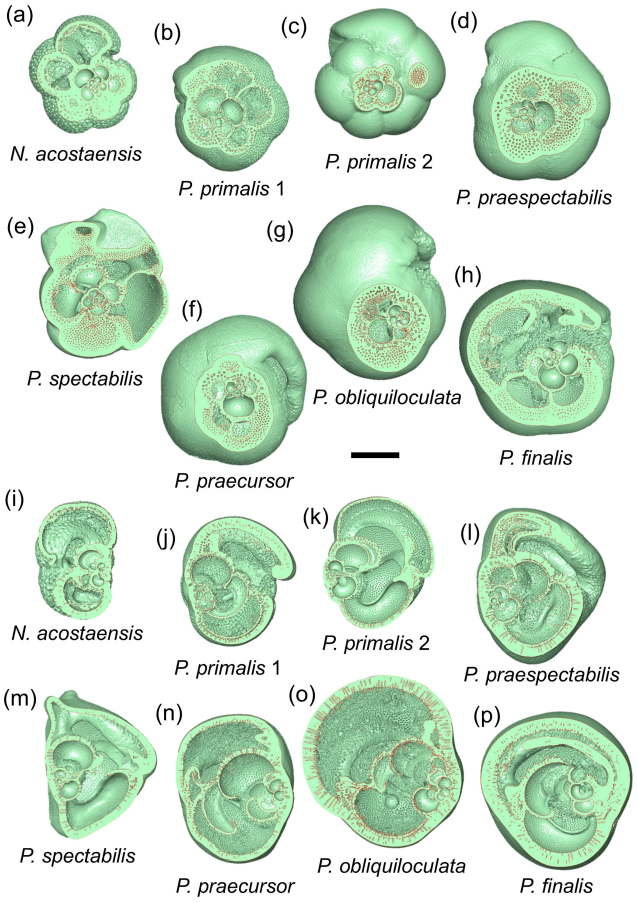

Figure 3. Cross-sectional cuts taken through the three-dimensional models through the proloculus in spiral view **(a–h)** and roughly orthogonally in side view **(i–p)**. The scale bar is 200 µm.

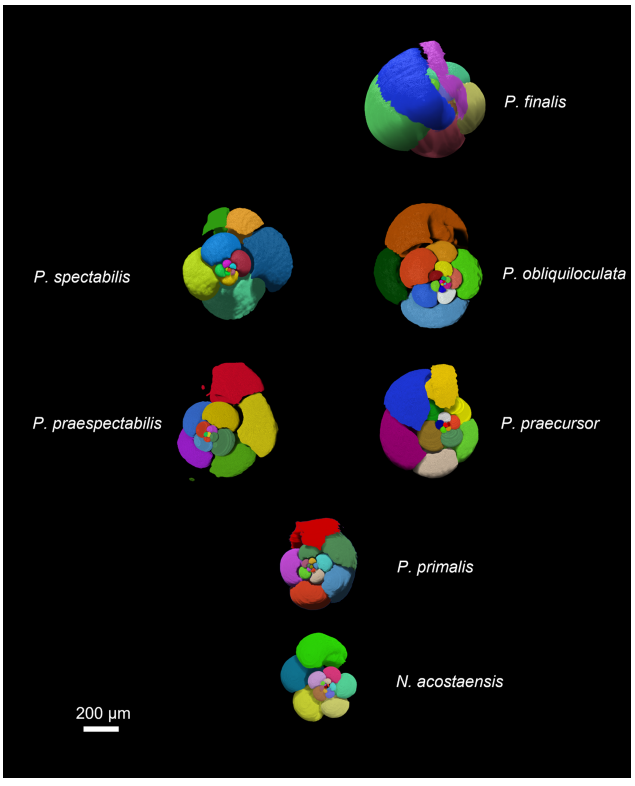

Figure 4. Chamber segmentation of representative specimens of the seven morphospecies. Note that the *P. primalis* specimen is *P. primalis* 1 from near the beginning of the stratigraphic range. The scale bar is 200 µm.

which produces a so-called "streptospiral" arrangement (literally, from the Greek, a twisted spiral). This is difficult to quantify because there is no consistent reference frame, so it is best visualized with the foram3D tool and described qualitatively.

Our specimen of *Neogloboquadrina acostaensis* has a test consisting of exactly three whorls (from the deuteroconch to the final chamber). The first whorl is very flat, in which the chamber centroids are added almost planispirally (Fig. 5h). Up to Chamber 6, the dorso-ventral axis is not well defined; therefore the coiling direction is not obvious from the centroid positions alone. Thereafter, the test follows a moderate trochospiral throughout its growth, except for the final chamber, which is positioned slightly backward along the direction of translation of the previous trochospire. This makes the centroid of the final chamber slightly nearer the proloculus than its predecessor. Irregular placement of this final chamber is related to the fact that it is slightly smaller than the penultimate chamber, a common feature of the adult phase in many planktonic foraminifera.

A coiling mode similar to *N. acostaensis* is seen in *Pulleniatina primalis*, with a flat inner whorl and more trochospiral arrangement after Chamber 6 (Fig. 5a, b, h, i). There are two fewer chambers than in *N. acostaensis* (16 instead of 18), and the test consists of about 2.75 whorls. The last 2 to 3 chambers are placed irregularly. This is related to size reduction and decreasing chamber aspect ratio in the adult phase, as discussed in the following subsections.

Pulleniatina praespectabilis and *P. spectabilis* have fewer chambers still (14 and 15 respectively). They become distinctly trochospiral earlier in their ontogeny than the other species, after Chamber 5 (Fig. 5j–k). The coiling is also tighter, with 4 chambers per whorl for much of the growth, giving the spirals a square rather than a pentagonal appearance. The pattern becomes more irregular in the final whorl because of small, flattened adult chambers, especially in *P. spectabilis*.

The remaining species (*P. praecursor*, *P. obliquiloculata*, and *P. finalis*) are even more irregularly coiled as adults and can be regarded as transitioning between three coiling modes: near planispiral in the initial whorl, then trochospiral, and finally streptospiral. Our specimen of *P. praecursor* has a virtually flat inner spiral up to Chamber 6, followed by a moderate trochospiral up to Chamber 10, after which

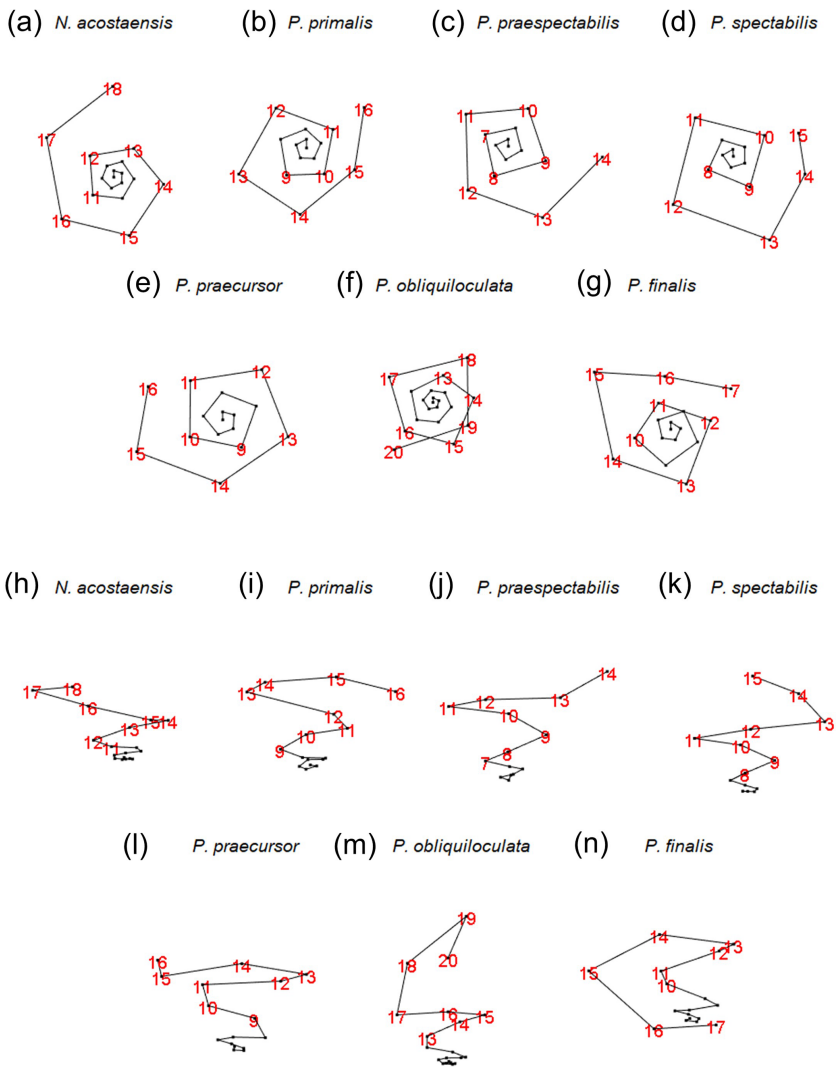

Figure 5. Visualization of the chamber centroids of the examined specimens using the foram3D package. Not to scale. Views in panels **(a)** to **(g)** are taken looking down the coiling axis from the spiral side. Views in panels **(h)** to **(n)** are taken roughly normal to the coiling axis. Chamber numbers are shown in red to visualize the last whorls.

the centroids of Chambers 11 to 15 are arranged almost in a plane with an axis at an angle of about 40° to the previous trochospire (Fig. 5e, l). These chambers are also strongly involute and increasingly compressed. The final chamber, Chamber 16, is highly vaulted, extending over the umbilicus, with a centroid slightly above the plane of the earlier chambers. The specimen of *P. obliquiloculata* is near planispiral up to Chamber 6 with a fairly regular trochospiral up to Chamber 14 (Fig. 5f, m). The subsequent chambers can be thought of as streptospiral, with the coiling axis increasingly tilted away from the earlier axis until the final chamber, Chamber 20, is added at an angle of about 90° to the initial axis (Fig. 5m). There are 3.5 whorls in total. The specimen of *P. finalis* begins with a nearly flat spiral up to Chamber 5 followed by a trochospiral phase up to Chamber 8. After that, the axis of coiling increasingly tilts away from its previous direction, eventually quite dramatically, so that the strongly involute chambers effectively grow back down the preceding spire, entirely enveloping the earlier test. The pseudoplanispiral outward appearance of the test is caused more by the fact that the aperture extends almost symmetrically over the periphery of the preceding whorl rather than being a truly planispiral arrangement of the chamber centroids, although we have observed other more extreme specimens of *P. finalis* that may better approach an effectively planispiral coiling mode in their last few chambers.

Morphometric data derived from the volume and position of individual chambers are plotted in Fig. 6. The volumes of individual chambers are shown in Fig. 6a. The proloculus is always larger than the deuteroconch (second-formed chamber), as is generally the case in planktonic foraminifera (Schiebel and Hemleben, 2017, and references

therein). Thereafter, most of the specimens show fairly constant chamber growth through ontogeny until the last few chambers, although, even in the main growth phase, the chambers are occasionally smaller than would be expected from a smooth progression. The incremental growth rate, defined as the internal volume of each new chamber divided by the sum of the internal volumes of all previous chambers, is shown in Fig. 6b. The data are quite "noisy", but there is a distinct contrast between specimens with a relatively constant growth rate (*N. acostaensis* and *P. obliquiloculata*) and those with accelerated growth in the middle phase (e.g. *P. praespectabilis* and *P. spectabilis*), during which time each new chamber is larger than the total preceding internal volume. The cumulative volume of all chambers is shown in Fig. 6c. Aspect ratios of successive chambers are shown in Fig. 6d. The proloculi are generally subspherical, and the deuteroconchs are always more compressed because they abut the rounded wall of the proloculus on one side. Thereafter, the early chambers are spheroidal, but aspect ratios frequently decline later in ontogeny, depending on the species. The chamber angles of each successive chamber are shown in Fig. 6e, beginning with Chamber 4, as the calculation depends on the position of earlier chambers. In general, the higher the chamber angle, the more chambers can be accommodated in a single whorl. Shown for reference are the internal chamber angles of a square, pentagon, hexagon, and heptagon which are 90, 108, 120, and 128.6° respectively.

The specimen of *Neogloboquadrina acostaensis* has a very small proloculus (long axis just 8 µm, volume 403 µm^3, Fig. 6a), and subsequent chambers remain smaller than their equivalent number chambers of all the *Pulleniatina* morphospecies throughout its growth. The rate of size increase is relatively constant, and the chamber angle is relatively steady, averaging 112°, such that the expanding helix contains almost exactly 5 chambers per whorl throughout growth (Fig. 6e). The chamber aspect ratio is also relatively constant, declining only slowly after Chamber 12 (Fig. 7d). These factors mean that *N. acostaensis* has a relatively self-similar morphology throughout ontogeny. The test has a total of 18 chambers, which is more than all the pulleniatinids except *P. obliquiloculata*, but the final size is considerably smaller than its descendants due to its succession of smaller chambers.

The specimen of *Pulleniatina primalis* differs from *Neogloboquadrina acostaensis* in several respects. Most obviously, the proloculus is much larger (long axis 14.5 µm, volume 2028 µm^3) and about average for *Pulleniatina* as a whole (see Fig. 6a). The rate of chamber increase is similar to *N. acostaensis*, but the test reaches an equivalent internal volume to the adult *N. acostaensis* after just 12 chambers then adds 4 more (Fig. 6a, b, c). The chamber angle is similar early on, producing 5 chambers per whorl, but reduces to an average of 102° from Chamber 9 to 15 which produces about 4.5 chambers per whorl (Fig. 6e). The placement of the final chamber is somewhat aberrant, resulting in 5 chambers in the final whorl (Fig. 6e). Another difference is that the chamber aspect ratio reduces much more quickly from Chamber 12 onward than in *N. acostaensis*. This is due to a combination of radial compression and increasing involution as the chambers become more highly vaulted over the umbilicus.

The selected specimens of *Pulleniatina praespectabilis* and *P. spectabilis* both have proloculi that are slightly larger than that of *P. primalis* and exhibit a distinctly faster chamber-by-chamber growth increase from Chamber 3 onwards (Fig. 6a, b, c). At Chamber 11, they both have a larger internal volume than all the other species at the same stage, but, at this point, the incremental growth rate slows as the chambers become radially compressed and develop their distinctive triangular shape. The last 2 chambers of *P. spectabilis* are flattened with little internal space. For much of their growth, they have a lower chamber angle which produces just 4 chambers per whorl in *P. spectabilis* and a little over 4 in *P. praespectabilis*. The chamber angle increases again for just the last 3 chambers, which are about the same volume as each other in *P. praespectabilis* and become progressively smaller in *P. spectabilis*. This late increase in chamber angle means that both forms have about 5 chambers in the final adult whorl (Fig. 6e).

The specimen of *Pulleniatina praecursor* exhibits a rather irregular increase in chamber volume through ontogeny, but, overall, the rate of chamber increase is similar to *P. primalis* (Fig. 6b, c). The aspect ratio of newly added chambers decreases sharply from Chamber 12 onward. The chamber angle averages 104°, which produces about 4.5 chambers per whorl, so it is overall more tightly coiled than *P. primalis*. The final whorl has 5 chambers, mainly because the final 2 chambers, which are added in a streptospiral arrangement, have slightly reducing volumes, similarly to the situation in *P. praespectabilis* and *P. spectabilis*.

The *Pulleniatina obliquiloculata* specimen has a relatively small proloculus and deuteroconch compared to other members of the genus (Fig. 6a), though still much larger than *N. acostaensis*. This, combined with a lower average chamber-to-chamber growth rate than all the other specimens, means that the volume increase per chamber lags behind the other pulleniatinids. Up to Chamber 17, the average chamber angle is a high 113° (Fig. 6e), producing slightly over 5 chambers per whorl. This reduces for the last 3 chambers in the streptospiral phase, resulting in just 4 chambers in the final whorl. The total chamber number is 20 (Fig. 6a), higher than all the other species, which average 16. Moreover, the last few chambers show no slowing in the rate of size increase. This eventually produces an internal volume that is about equal to *P. finalis* and higher than all the other morphospecies (Fig. 6c). The chambers increase in volume mainly because the test remains quite evolute, and the chambers are globular, with only a slow reduction in their aspect ratio and little radial compression.

The *Pulleniatina finalis* specimen has by far the largest proloculus (long axis 21.9 µm, volume 6867 µm^3) and deute-

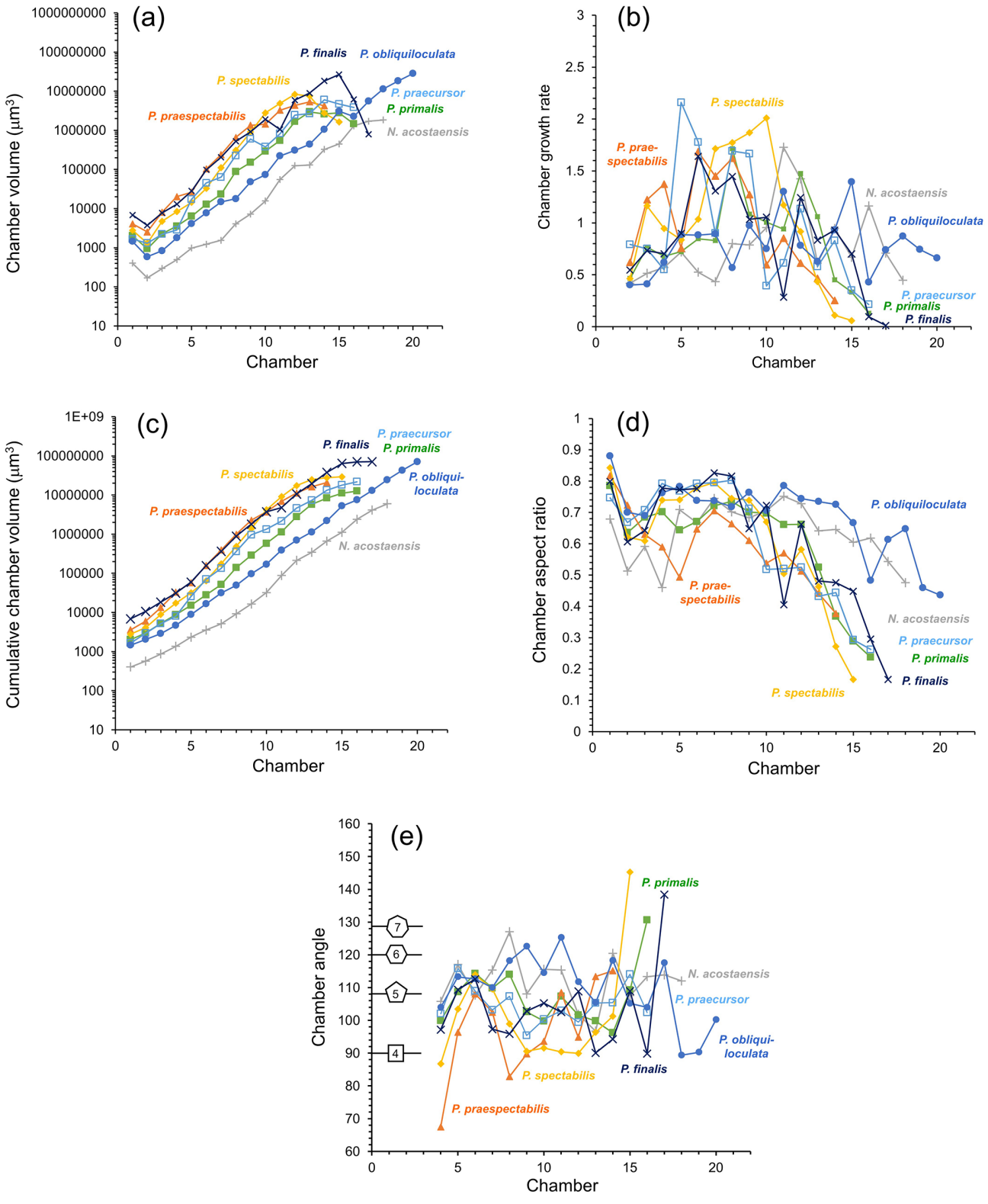

Figure 6. Morphological data as a function of chamber number. **(a)** Chamber volume, **(b)** chamber growth rate (ratio of chamber volume to total previous chamber volumes), **(c)** cumulative chamber volume, **(d)** chamber aspect ratio, **(e)** chamber angle. Shapes indicate the internal angle of regular polygons for reference.

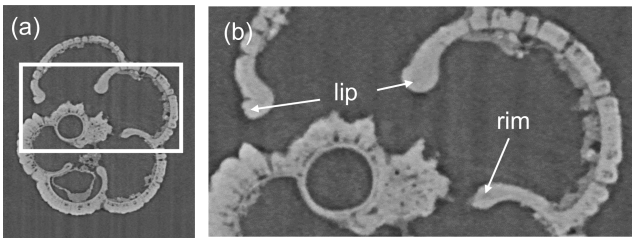

Figure 7. **(a)** Example of a reconstructed slice of *Neogloboquadrina acostaensis* in equatorial section. **(b)** Enlarged view showing additional thickening of the area around the aperture to form the apertural rim and adult lip characteristic of the species. The thickening is a non-porous X-ray dense (opaque) "modification layer" (see text for discussion).

roconch (Fig. 6a). Up to Chamber 15, the incremental size increase is a little faster than both *P. praecursor* and *P. obliquiloculata* despite the fact that the aspect ratio declines from Chamber 10 onward as the chambers become progressively more involute (Fig. 6b, e). The last 2 chambers are highly aberrant, being little more than anterior extensions to the antepenultimate chamber with very small internal volumes (Fig. 6a). The internal spaces in the adult *P. finalis* are very cramped because of these reduced chambers combined with the thick walls and involute coiling.

3.4 Test layering

The raw X-radiographs and the three-dimensional mesh models reveal how the test is constructed from successive layers. As described above, our specimen of *Neogloboquadrina acostaensis* has a rather generalized morphology caused by consistent chamber shape and growth. Its most interesting feature is the modification of the aperture in the adult form (Fig. 7). Earlier chambers have a relatively simple arched rim around the aperture, but this develops an anterior-directed curvature on the last 2 chambers only, forming a projecting lip. The lip is irregular along its length but is clearly seen from the exterior, which is a characteristic feature of the species (see Fig. 2). It is evident from the X-radiographs that the apertural rims and lip are thickened by a smooth external layer that appears slightly denser (more opaque) than the wall in general and wraps around the aperture.

Features that are typical of the *Pulleniatina* group are explored in Fig. 8 using *P. primalis* 2 as an example. The X-radiographs clearly show that the test is layered, with pores covering most of the inner surface and extending upward through much of the test wall but with an outer non-porous layer (cortex) that appears white (X-ray dense) and covers the entire external surface. As in *N. acostaensis*, where successive chambers meet at the sutures, the inner layer of each new chamber can be seen terminating against the preceding chamber, whereas outer layers continue over the suture in a contiguous manner, with the pre-existing pores extending upward through these new layers (Fig. 8c). This feature of the wall can also be seen in some of the earlier published thin section images (e.g. Brady, 1884; Postuma, 1971). The cortex is largely non-porous, although, in some places, the pores can be seen to diminish upward through it. The chamber walls in the later ontogenetic stages become strongly recurved in the apertural region, forming an inwardly directed apertural face. There is no forward-curved apertural lip as described above for the adult *N. acostaensis*. Nevertheless, on each adult chamber, the apertural rim is locally thickened on both sides by an additional non-porous smooth layer that terminates inside the test near the point of maximum curvature (similar to that seen on the earlier chambers of *N. acostaensis*). This localized structure appears to be a distinct architectural element deposited around the aperture after initial chamber formation and is referred to here as a "modification layer" because it is deposited only locally and does not extend over the whole chamber. Interior views of the 3D models show very clearly how the internal foramina are rimmed by this smooth non-porous modification layer (Fig. 8e–f). The cortex also wraps around the apertural face, meaning that, for the final chamber only, there are two dense layers wrapping around the aperture (Fig. 8b).

3.5 SEM investigations

Although representative specimens of all *Pulleniatina* morphospecies were crushed and examined under SEM, the clearest results were obtained from the two extant forms, *P. obliquiloculata* (Fig. 9) and *P. finalis* (Fig. 10), because the older material is degraded by diagenetic recrystallization (Rosenthal et al., 2018). Of particular note in these images is the layering of the wall and the contrast between the microgranular textures of the main test wall with the dense bladed crystal structure of the cortex. It is also possible to see how the pores come close to the test surface, where they are closed by radial sheets of cortex. This accounts for the observation that the pores are clearly visible through the transparent wall in light microscope imaging (see Fig. 9a).

The crushed *P. obliquiloculata* highlights a fragment of the penultimate chamber wall viewed from the inside (see Fig. 9f and g). The pores of this chamber all constrict at the level of the primary organic sheet (POS), which may have originally extended drum-like across each pore, forming a structure called a "pore plate" (Hemleben et al., 1989). The innermost test layer below this level is the primary layer (PL) highlighted in Fig. 9g. Several other layers of microgranular calcite can be seen rather faintly in the pore walls, probably constituting two secondary layers and four adult layers. Above this is the cortex (CX), which consists of large, solid-bladed crystals. Prior to cortex formation, the test wall was porous with weak inter-pore ridges, hence the undulose join highlighted in Fig. 9g. The pores are closed off by the cortex with inward-growing radial sheets of calcite which coalesce upward to form a flat, smooth external surface. Similar ap-

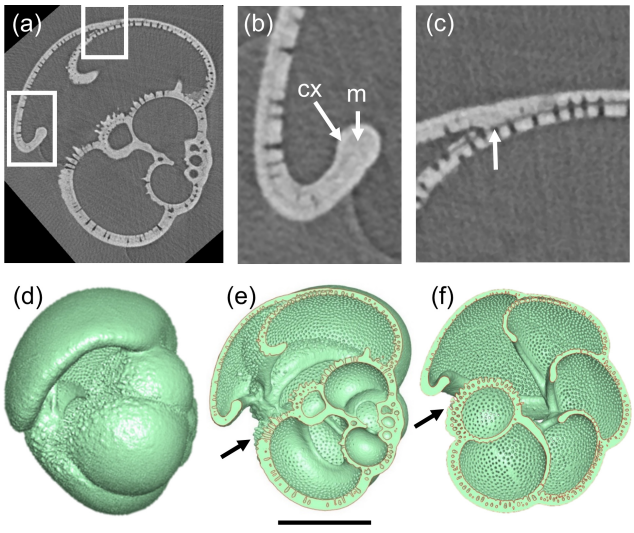

Figure 8. Investigation of test layering in *P. primalis* 2. **(a)** X-radiograph of the specimen in side view showing the porous test wall and the high-density non-porous outer layer (cortex). Boxes show areas highlighted in subsequent images. **(b)** Detail of the final chamber, showing the recurved chamber wall forming an apertural face. Arrow "m" shows a smooth thickened area around the apertural face interpreted as a "modification layer" (see text), which is overlain by the cortex "cx", which wraps around the apertural flap as far as the inner reflex angle and externally over the whole surface. **(c)** Detail of the attachment of the final chamber showing how the primary layer terminates at the chamber junction (white arrow) while the secondary layer and cortex continue to cover the entire outer test surface. **(d)** Mesh model in side view, for reference. **(e)** Cross-section through the mesh model corresponding to the X-radiograph, revealing the non-porous apertural lips (modification layers) on the inner and outer surfaces of the apertural faces. The secondary layer and cortex of the final chamber thicken all the chambers as far as the area below the aperture, highlighted with an arrow. **(f)** Cross-section in equatorial view looking down into the porous inner surfaces of the vaulted chambers around the umbilicus. The secondary layer and cortex of the final chamber thicken all the earlier chambers of the final whorl as far as the area below the aperture (arrow). The internal septa are composed of thin bilamellar units covered around the apertures (foramina) with a smooth "modification layer". The scale bar is 200 µm.

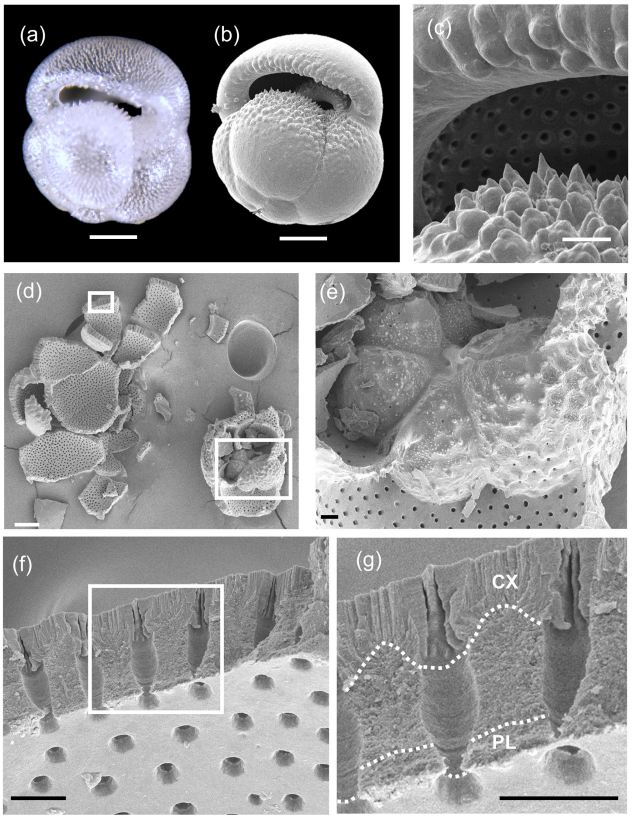

Figure 9. SEM investigation of crushed test of *Pulleniatina obliquiloculata* from Sample 363-U1488A-1H-2, 80–82 cm. **(a)** Multifocus light microscope image, clearly showing the subsurface pore channels. **(b)** SEM image showing the smooth outer cortex; scale bar 100 µm. **(c)** Detail of pustules above and below the aperture; scale bar 20 µm. **(d)** Results of crushing, with boxes highlighting the areas of subsequent images; scale bar 100 µm. **(e)** Detail of inner whorl showing the juvenile morphology; scale bar 10 µm. **(f)** Wall of penultimate chamber in cross-section, with the box highlighting the area of subsequent image; scale bar 10 µm. **(g)** Detail of wall in cross-section; scale bar 10 µm. Dotted lines separate the primary layer (PL) and the cortex (CX) from the intervening secondary and adult layers. The subtle wall layering is best seen in the pore channels.

pearances can be seen on the crushed *P. finalis* (see Fig. 10c). In this fragment, interpreted as part of the penultimate chamber, the primary layer has detached completely during crushing along the POS, which forms the inner surface of the fragment. The secondary layer (SL) has partly divided from the rest of the test to open up a small gap between it and the layer above (AL1), followed by what appears to be five microgranular adult layers that thicken the wall considerably, above which is a cortex similar in appearance to that seen in *P. obliquiloculata* (see Fig. 9g).

The test structure of *P. obliquiloculata* was recently studied by Lastam et al. (2023a, b), who examined specimens embedded in resin and etched with weak acid. Those authors noted a difference between blocky crystallites that form the primary layer and more fibrous forms in the overlying secondary and adult layers, a distinction that is not obvious in our un-etched specimens. The constriction of the pores at the level of the POS is clearly visible in their images (e.g. Lastam et al., 2023b, their Fig. 1e). Lastam et al. (2023a, b) used electron backscatter diffraction (EBSD) analysis to demonstrate that the microgranules which grow upward from the POS constitute large crystallographically oriented and twinned domains that extend through much of the wall, including running across successive layers. Similar results were described by Procter et al. (2024) for an-

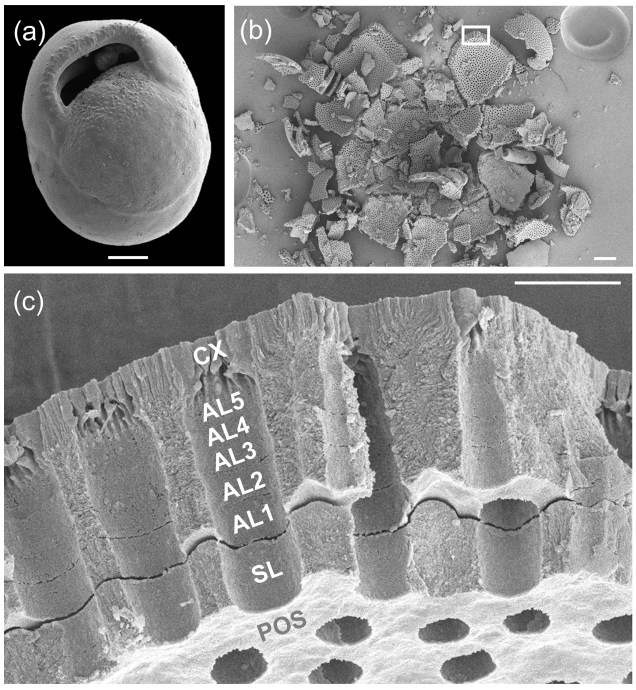

Figure 10. SEM investigation of crushed test of *Pulleniatina finalis* from sample U1488A-1H-2 (80–82 cm). **(a)** SEM image; scale bar 100 µm. **(b)** Result of crushing, with the box highlighting the area of the subsequent image; scale bar 100 µm. **(c)** Detail of the final chamber wall in cross-section; scale bar 10 µm. In this image, the primary layer has broken off during crushing at the level of the primary organic sheet (POS), which forms the inner surface of the fragment, and a small gap has opened between the secondary layer (SL) and the subsequent adult layers (AL1-5) and cortex (CX).

other modern species, *Globigerinoides ruber*, and an extinct Eocene form, *Morozovella crater*. Whether these domains can be considered "crystals" in the conventional sense is a moot point given their highly irregular fibrillar/granular structure, intimate intergrowth with a biopolymer network, and extension across successive internal secondary and adult layers that were formed episodically during growth (see Discussion in Procter et al., 2024).

4 Discussion

4.1 Growth model

The pattern of test layering accords well with the classic "bilamellar" model proposed by Reiss (1957), as modified by Fehrenbacher et al. (2017) and Pearson et al. (2022), to accommodate adult layers that are not associated with chamber growth. The model is further extended here in Fig. 11 to allow for the smooth "modification layer" around each newly formed apertural rim or flange. In this model, each new chamber is formed initially from two layers separated by a primary organic sheet (POS) (alternatively, primary organic membrane; e.g. Kunioka et al., 2006). The inner primary layer is generally thinner than the outer secondary layer. Together, these make a structural element called a bilamellar unit. However, while the primary layer and the POS terminate at the join (suture) with the preceding chamber, which is generally high above the aperture, the secondary layer extends over the entire external surface of the test, terminating below the newly formed aperture on the first chamber in the whorl. In this way, the secondary layer associated with each chamber attaches it to the rest of the test and thickens all the chambers of the final whorl externally (see also Kunioka et al., 2006). The last stage in the formation of the final chamber, according to our revised model, is the secretion of a smooth modification layer which wraps around both sides of the apertural face, covering the pores. In the adult stage, additional test layers can be laid down without new chambers being formed. In the terminal stage of the life cycle, a special kind of adult layer, termed a "gametogenic" layer, can be laid down (Bé, 1980). The cortex in *Pulleniatina* seems to be a specialized type of gametogenic layer peculiar to the genus, although a direct association with gametogenesis has yet to be demonstrated in vitro. The gametogenic layer can cover the entire external surface, and, in the case of *Pulleniatina*, it also wraps around the inner surface of the apertural face of the final chamber (see Fig. 8b).

4.2 Ontogeny

In this subsection, we interpret aspects of the growth and development of *Pulleniatina* and its supposed ancestor *Neogloboquadrina acostaensis* based on the growth model of Brummer et al. (1987), which includes five ontogenetic stages: prolocular, juvenile, neanic, adult, and terminal. Although this model was initially developed for spinose species, we find it applicable to *Pulleniatina*, although the transitions between juvenile, neanic, and adult stages are more gradual than seen in some spinose species.

4.2.1 Prolocular stage

The first-formed chamber of a foraminifer is conventionally called the proloculus. The stage of the life cycle from cell formation by sexual reproduction (i.e. fusion of gametes to form a zygote) up to construction of the proloculus is termed the "prolocular stage" (Brummer et al., 1987). This phase of the life cycle must involve initial feeding and cell growth because the proloculus is proportionally much larger than the gametes. The sizes of proloculi differ markedly among different species of planktonic foraminifera, with those of *Pulleniatina* reported as being among the largest, with a mean diameter of 23 µm and a total range between 14 and 31 µm ($n = 36$) (Sverdlove and Bé, 1985). The diameters of the proloculi as measured in our study are an average of 16 µm, hence smaller than reported by Sverdlove and Bé (1985), although it is difficult to draw conclusions from the small sam-

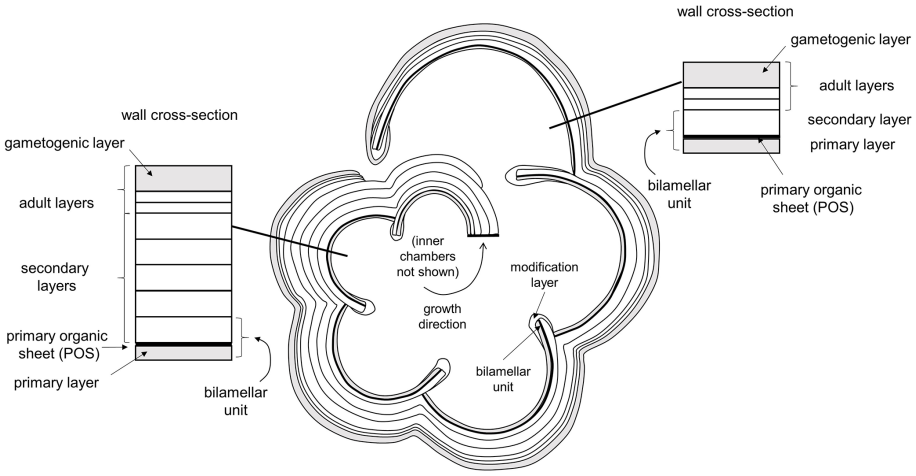

Figure 11. Model for shell layering in planktonic foraminifera based on Reiss (1957), modified by Fehrenbacher et al. (2017) and Pearson et al. (2022) and herein. This example has three adult layers not associated with chamber formation (the number is arbitrary), including one terminal gametogenic layer (in *Pulleniatina*, the cortex).

ple size ($n = 6$). Also, our proloculus data are based on the inner volume rather than the external measured size, which also includes an organic capsule that may be lightly calcified (Meilland et al., 2023). In the micro-CT data of Darling et al. (2023), the mean internal proloculus size of modern *Neogloboquadrina pachyderma* (a relative of *Pulleniatina* adapted to sub-polar and polar waters) is 16.5 µm, similar to our data for *Pulleniatina*.

Our micro-CT scans have a resolution of 0.5 µm, which is too large to resolve any features of the proloculus other than their general shape, which is always a globular spheroid with an aspect ratio between 0.65 and 0.9. Meilland et al. (2023, their Fig. 2j) illustrated a small circular aperture on an asexual megalospheric proloculus produced in vitro, but we cannot confirm the presence of apertures (foramina) on our specimens or indeed the first few chambers of the juveniles. Nevertheless, we presume they must have existed for cytoplasm connectivity.

While most planktonic foraminifera have often been considered to exclusively reproduce sexually (e.g. Hemleben et al., 1989; Schiebel and Hemleben, 2017), work on *Neogloboquadrina pachyderma* has demonstrated the presence of a biphasic life cycle with an asexual phase (Kimoto and Tsuchiya, 2006; Davis et al, 2020; Darling et al., 2023; Meilland et al., 2023). This produces a dimorphism in proloculus size within the species, in which individuals with large proloculi (so-called "megalospheric" forms) are the product of asexual reproduction and those with small prolocuili ("microspheric" forms) are the product of sexual reproduction (Meilland et al., 2023). While many benthic foraminifera exhibit obligate alternation of asexual and sexual generations, this does not seem to be the case for *N. pachyderma*, wherein the asexual reproductive strategy may be adventitious, determined by environmental conditions and population size (Meilland et al., 2023). It has also been noticed that megalospheric forms can exhibit anomalous coiling directions relative to their parent and the population at large, which happens to be strongly dominated by sinistral coiling in *N. pachyderma* (Kimoto and Tsuchiya, 2006; Meilland et al., 2023; Darling et al., 2023). Asexual reproduction has also been observed in some phylogenetically unrelated microperforate species of planktonic foraminifera (Takagi et al., 2020) but has so far not been observed in spinose species or tropical non-spinose forms including *Pulleniatina*. It is currently unclear whether *Pulleniatina* ever reproduces asexually and, if so, how frequently. Anomalous coiling directions in modern *Pulleniatina* are extremely rare – the entire global population seems to be exclusively dextral, except for very low numbers of sinistrals reported in just one study (Brummer and Kroon, 1988).

We noted quite a large and unexpected discrepancy in proloculus size between our core top specimens of *P. obliquiloculata* (13 µm) and *P. finalis* (22 µm). To investigate this further, we imported the CT scans published by Chen et al. (2023) from ODP Hole 1115B in the western tropical Pacific into OS Dragonfly to measure their proluculi. These comprise the morphospecies *P. finalis* (3 specimens), *P. obliquiloculata* (14 specimens), and *P. praecursor* (3 specimens). However, of these, we were only able to measure four prolocuili successfully, as shown in Table 2. Despite the small sample size, a clear pattern emerges, with the *P. finalis* prolocuili being much larger on average (8063 µm^3, $n = 3$) than those *P. obliquiloculata* (1820 µm^3, $n = 2$) or all other species combined (2288 µm^3, $n = 6$), with a high significance level even with the original data that prompted the enquiry removed. This finding suggests either (1) that the *P. finalis* morphospecies is part of the same general population as *P. obliquiloculata* but comprises individuals that happen

to have large proloculi and, as a consequence, large chamber volumes throughout ontogeny, the accommodation of which causes the characteristic test of the adult stage; that (2) *P. finalis* is an asexual megalospheric variant of *P. obliquiloculata* with an aberrant morphology; or that (3) *P. finalis* is a distinct biological species which has hitherto been lumped with *P. obliquiloculata* in biological and genetic studies. These possibilities are best resolved with new observations on living specimens in culture or genetic studies.

4.2.2 Juvenile stage

The ontogenetic stage from the deuteroconch up to about 7 chambers has been called the "juvenile stage" (Brummer et al., 1987). In each of our specimens, the deuteroconch is about 70 % of the size of the proloculus by maximum length and 40 % by volume (see Fig. 6a). The third chamber is always larger than the deuteroconch and can be either larger or smaller than the proloculus depending on the specimen. Chamber growth thereafter follows a roughly logarithmic pattern (although with departures, as discussed below). Thus, for much of the growth, the size of the test after a given number of chambers is largely determined by the size of the deuteroconch. There are, however, slight differences in chamber-by-chamber growth rate between species, as discussed further below.

The placement of the third chamber relative to the previous two generally reveals the orientation of the growing spiral, including the plane of coiling and the anterior/posterior orientation of the chambers, wherein the anterior chamber faces point away from the previous chambers. The aperture is positioned at the base of the anterior chamber face, although it is usually unresolvable in our micro-CT scans for the first few chambers. Each successive chamber is attached above and around the pre-existing aperture and extends forward and arches down onto the previously formed part of the test on either side of a newly formed aperture. The chamber angle (defined as the line between the centroids of the new chamber and the previous one; Brombacher et al., 2022) is always less than 180°, which has the effect of making the test coil forward onto itself in a spiral arrangement. The coiling direction (dextral or sinistral) is determined by the direction of translation of the growing spiral relative to the general plane of coiling. The coiling direction may not become clear immediately because the spiral can be very flat initially and the chambers are generally quite spherical. The spiral can even appear to reverse its direction of translation, as happens, for instance, in our specimen of *N. acostaensis* after the first few chambers (see Fig. 5h).

The chambers of the early whorl are subspherical, generally with an aspect ratio of about 0.7. Compression is radial, such that chambers are shorter in the radial direction and higher in the dorso-ventral direction. However, as ontogeny progresses, there is also a tendency for the anterior faces of chambers to become increasingly flattened above and around the apertures (foramina). The apertures, where visible, are nearly circular and generally surrounded by a rim or lip. The early chambers have few pores, with pores focused on the spiral side, and the chamber surfaces are covered in small conical pustules (see Fig. 9e). It has been suggested that the conical pustules in the juvenile may be spine bases (as shown in the elegant dissections of Burt and Scott, 1975). This is possible, given that the supposed Miocene ancestor *Paragloborotalia* was sparsely spinose (as discussed by Leckie et al., 2018, p. 126), but we have been unable to confirm the presence of embedded spines in any of our dissections, and they certainly do not occur in the later ontogenetic stages.

The juvenile stages of all our specimens are remarkably similar despite belonging to different morphospecies. This may be because the tests are very small and generalized, and the micro-CT does not resolve ultra-fine features, but it may also point to a common and conservative life habit in the early stages of development. This suggests that juveniles had similar feeding strategies, possibly grazing bacteria, whereas adults may have diverged into different specialisms associated with their respective ecological niches.

4.2.3 Neanic stage

According to the model of Brummer et al. (1987), spinose planktonic foraminifera typically transition from a juvenile to "neanic" (from the Greek word for "youthful") stage at about the seventh chamber. This transition seems to be more marked in spinose than non-spinose species, where it is associated with major changes in trophic strategy and morphology. However, it is also a useful concept in the case of *Pulleniatina* because it is around this stage that morphological divergences between the different species begin to become apparent. It is also around this stage that the test transitions from a flat spiral to a distinct trochospire and the chambers becomes variously more compressed (lower aspect ratio), depending on the morphospecies (see Fig. 6c). The chambers become larger and extend further onto the umbilical side, and, in most species, the trochospirality steadily increases thereafter (see Figs. 5 and 6). The neanic stage tends to correspond to the largest chamber-to-chamber growth rate, as the cell presumably focuses all its resources on feeding and growth.

From the neanic stage onward, the basic wall structure of *Pulleniatina* is weakly cancellate, in which regularly spaced pores are set within raised inter-pore ridges, recalling the supposedly ancestral wall texture of *Neogloboquadrina acostaensis*. All planktonic foraminifera have such pores, albeit with different sizes and densities (e.g. Fabbrini et al., 2023), although their precise function has yet to be determined (Schiebel and Hemleben, 2017). Most likely they regulate ion exchange across the thin organic membrane (pore plate) set deep within the pore channels (Bé et al., 1980). While pores in the juvenile stage can be rather sporadic and often situated in the sutural areas, in the neanic stage, the

Table 2. Summary of proloculus size data measured from the micro-CT scans of Chen et al. (2023) and this study.

Reference	Morphospecies	Sample	Aspect ratio	Volume (μm^3)
Chen et al. (2023)	*P. finalis*	1115B/12H-6, 65–67 cm	0.800	8609
Chen et al. (2023)	*P. finalis*	1115B/12H-6, 65–67 cm	0.784	8713
Chen et al. (2023)	*P. obliquiloculata*	1115B/13H-6, 95–97 cm	0.924	2182
Chen et al. (2023)	*P. praecursor*	1115B/13H-4, 5–7 cm	0.941	1494
This study	*P. finalis*	U1488A/1H-2, 80–82 cm	0.799	6867
This study	*P. obliquiloculata*	U1488A/1H-2, 80–82 cm	0.881	1458
This study	*P. praecursor*	U1488A/9H-CC	0.747	1651
This study	*P. spectabilis*	U1488A/12H-CC	0.843	2793
This study	*P. praespectabilis*	U1488A/16H-4, 80–82 cm	0.817	3582
This study	*P. primalis*	U1488A/20H-4, 81–83 cm	0.785	2028

wall structure tends to become more regular and organized. Pustules become larger and tend to be concentrated on the chamber surfaces below the aperture. These may serve to anchor the rhizopodial network associated with food gathering, such as harvesting algae from the surrounding environment.

4.2.4 Adult stage

The onset of the adult stage can occur after differing numbers of chambers depending on the species and individual. The adult stage in most species is associated with a distinct reduction in the aspect ratio and in the rate of chamber size increase for the last few chambers of the final whorl (see Fig. 6a). The chamber shape may become strongly modified, as seen most clearly in *P. spectabilis*, which develops an increasingly pinched periphery in the chambers of the final whorl. Other species-specific aspects of chamber addition (involution, streptospirality) become more marked in the adult chambers; hence the various morphospecies become more readily distinguishable. The morphology around the aperture can also develop, perhaps related to specialization of feeding strategies. For instance, one of the most distinctive features of the supposedly ancestral form, *Neogloboquadrina acostaensis*, is the prominent adult apertural lip which is visible externally (see Fig. 2). The lip on the final chamber is an imperforate rope-like band that rims the entire aperture, terminating adjacent to the umbilicus. There is a tendency for the pore pits and rims of the cancellate structure to become more smoothed out and for the pustules to become larger and more frequent. Below the aperture, they tend to be sharp conical projections, whereas, on the chamber face above the aperture, they tend to be more like blunt ovate mounds.

Chamber addition eventually ceases altogether in the adult stage, but the test can still be augmented by the addition of one or more external layers of calcite. This is most clearly seen in species such as *Orbulina universa*, where the final adult spherical chamber is thickened layer on layer over several days in what appears to be a day/night cycle (Fehrenbacher et al., 2017). The same probably occurs in *Pulleniatina*, wherein several adult layers (we have observed up to 5) are added to the test without ongoing chamber formation (see Fig. 9c).

4.2.5 Terminal stage

The terminal stage in planktonic foraminifera is generally associated with sexual reproduction, wherein cell function switches from feeding and growth to gamete production. It is advantageous for individuals to coincide gamete release in space and time with the rest of the population to maximize the chances of gamete fusion. The timing may be associated with the lunar cycle (Berger and Soutar, 1967; Spindler et al., 1979; Reiss and Hottinger, 1984; Schiebel et al., 1997; Jonkers et al., 2015), and individuals may migrate to a specific water depth or density, which generally involves descending through the water column. In many species, the terminal stage is associated with a major re-modelling of the test. In spinose species, the spine array can be shed and a thick layer of "gametogenic" calcite can be laid down. Shedding spines reduces drag, and the gametogenic crust may help increase test density and facilitate sinking (Bé at al., 1980).

In *Pulleniatina*, the terminal stage is marked by the laying down of the cortex: a dense, smooth, and largely non-porous external layer. Although some other species also have a similar terminal layer, also called a cortex (e.g. *Sphaeroidinella dehiscens*) in its particular morphology, the structure of the cortex in *Pulleniatina* is unique to the genus and is its defining feature. The cortex covers the pre-existing mural pores, giving the test a reflective, shiny appearance. The pustules are also overlaid by the cortex, although they may not be entirely smoothed out, making a lumpy appearance especially around the aperture. The high density of the cortex suggests that it exists in part to facilitate sinking. It is suggested here that the cortex of *Pulleniatina* may have evolved as a specialized development of the localized smooth "modification layer" that was laid down around the aperture and over the pores of each succeeding chamber in the supposed ancestor, *Neogloboquadrina acostaensis* (see Fig. 7). *Pulleniatina* also has the same kind of structure on every adult chamber. The

cortex may be a second such layer that, uniquely, extends from inside the aperture to cover over the entire external surface of the test. By this hypothesis, the modification layer may have evolved first in *Neogloboquadrina* or possibly a more remote ancestor. Its adaptive function is presumably to bridge over the pores and strengthen the aperture, but it was only with the evolution of *P. primalis* that the same cellular mechanism was re-purposed as an enveloping terminal layer. In most other species of planktonic foraminifer, the pores remain open despite the gametogenic layer. In *Pulleniatina*, the way in which the pores are closed by overhanging ribbons of calcite that grow outward from around their circumference (see, for example, Fig. 10c) seems to indicate that closure of the pore channels appears to be part of the primary function of the cortex. Whatever task the pores normally perform during growth, and in the adult stage, is evidently unnecessary and possibly disadvantageous in the terminal stage. Gamete release must be directed through the primary aperture because it is the only orifice available. After this, the cell dies and the life cycle begins again.

4.3 Phylogeny

The specimens included in this study are spread over more than 6 million years of geological time. While *Pulleniatina* was initially regarded as a monospecific genus of uncertain wider affinities (e.g. Cushman, 1927; Bolli et al., 1957), intensive study of fossil populations beginning in the 1960s has revealed details of its origin and evolution. The literature on the stratigraphic and geographic coverage of *Pulleniatina* morphospecies was summarized by Pearson et al. (2023), and an evolutionary model is illustrated in Fig. 12.

4.3.1 Origin of *Pulleniatina*

Most authors since Banner and Blow (1967) have regarded *Neogloboquadrina acostaensis* as the likely ancestor of the *Pulleniatina* clade. Evidence for this is based partly on their various shared characteristics, their overlapping stratigraphic ranges, and the existence of putative intermediate forms between *N. acostaensis* and *P. primalis*. It remains the case, however, that *P. primalis* appears rather abruptly in the known fossil record of the tropical Indo-Pacific at 6.50 ± 0.1 Ma (Pearson et al., 2023) and that the existence of a full range of intermediates has not been adequately demonstrated. The so-called intermediate specimens illustrated by Banner and Blow (1967) fall within the known morphological range of *P. primalis* (in our opinion). The curious specimen selected by Brönnimann and Resig (1971) to typify their morphospecies *Pulleniatina praepulleniatina* appears to be an aberrant form of *N. acostaensis* on account of its distinct apertural lip which is typical of that species but does not occur in *Pulleniatina*. Belyea and Thunell (1984) conducted a morphometric study that purported to document the transition from *N. acostaensis* to *P. primalis*, but their stratigraphic sampling was such that it is doubtful if a full continuum was demonstrated.

To further investigate the evolutionary origins of *Pulleniatina*, we studied the very earliest assemblage of *P. primalis* in our collection from IODP Site U1488, sample U1488A-21H-6, 9–11 cm from 193.99 m below sea floor (m b.s.f.). *Pulleniatina* is rare, and only 25 specimens were observed in the sample. The next sample down, Sample U1488A-21H-CC at 196.29 m b.s.f., lacks *Pulleniatina*. The putative ancestral species, *N. acostaensis*, is common in both samples and persists down-core through at least another 100 m of sediment. Some representative specimens from Sample U1488A-21H-6, 9–11 cm, are illustrated in Fig. 13 to a common scale. The *N. acostaensis* specimen illustrated (Fig. 13aa–ac) is a typical adult form with a reduced "kummerform" final chamber and a prominent apertural lip which forms a flat structure attached to the final chamber extending into the umbilicus. It is considerably smaller than the *Pulleniatina* specimens, as are all the *N. acostaensis* present. It is dextrally coiled, like 35 % of the *N. acostaensis* in the sample, which contrasts with the exclusively sinistral *Pulleniatina* assemblage. The *Pulleniatina* assemblage includes specimens without a cortex (Fig. 13e and g), presumably individuals that did not reach gametogenesis, but these are readily distinguished from *N. acostaensis* because they are larger and lack the umbilical lip/plate. The *P. primalis* mostly have 4.5 chambers in the final whorl, although some have 4. The final chambers tend to lean over the umbilicus (to varying degrees), unlike *N. acostaensis*. The cortex on some of the specimens, when present, appears incomplete, with the porous wall visible around the umbilical region (Fig. 13ba and ca) and in some cases in patches on the spiral side (Fig. 13be). The *Pulleniatina* specimens at this early stage are atypical of later *P. primalis* in that they are less compact. They show greater morphological similarity to *N. acostaensis* than later forms, but there is not a full range of intermediates. The possibility of a migration of early *Pulleniatina* into the Western Pacific Warm Pool cannot be excluded without investigating the 2.3 m sampling gap at Site U1488 and documenting eventual intermediate forms *N. acostaensis – P. primalis*.

These observations support the hypothesis that *N. acostaensis* and *P. primalis* are closely related, but the evolutionary transition has not been observed. Aside from the genus-defining cortex, *P. primalis* has a much larger proloculus than *N. acostaensis* and exhibits a clear transition from the neanic to adult stage in which the rate of chamber size increase declines (Fig. 6a, b, d) and the morphology of the chambers changes markedly, with later chambers typically leaning over the umbilicus (Fig. 2). In contrast, the growth of *N. acostaensis* is more self-similar into the adult stage. The main adult feature of *N. acostaensis* is the development of a large apertural lip, but this is not seen in *Pulleniatina*. Hence, it seems that, if *P. primalis* evolved from *N. acostaensis*, it required a suite of modifications from the proloculus through to the adult stage of ontogeny. It also appears to have involved

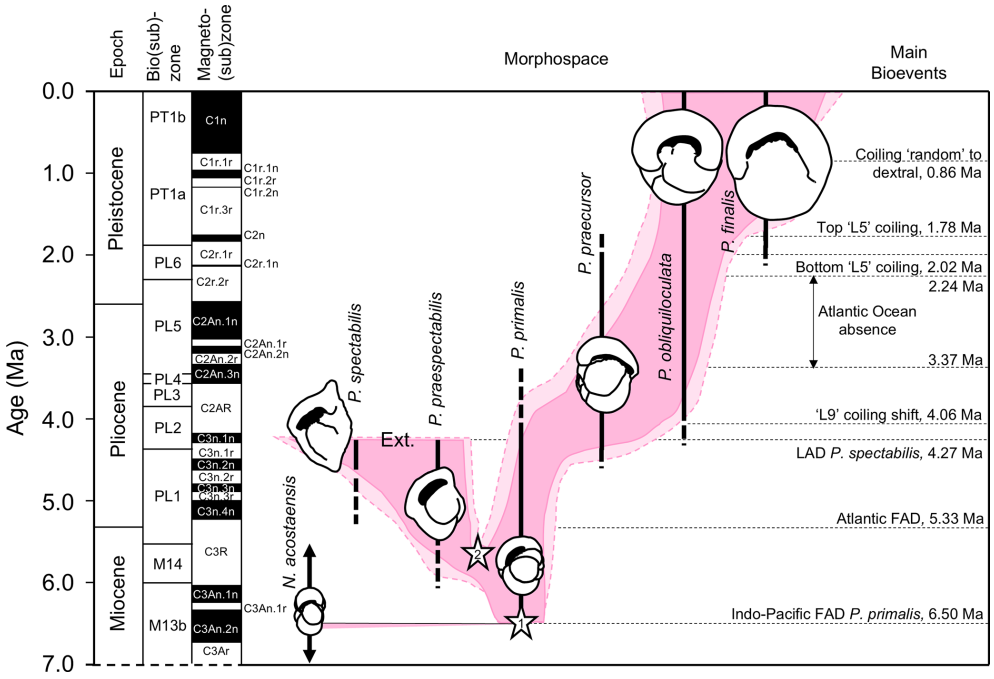

Figure 12. Model for the evolution of *Pulleniatina* showing proposed relationships between the various morphospecies as part of two evolutionary lineages. The shaded field is an interpretation of the way the genus has evolved through morphospace, as divided into six formally named morphospecies. Lighter shading represents age uncertainty. Cartoons are based on the holotype specimens and are approximately to scale. Cladogenetic events are shown with stars: the split between the *N. acostaensis* and *Pulleniatina* clade (1) and the split between the *spectabilis* and main lineages (2). "Ext." represents the sharp extinction involving the two species in the mid-Pliocene. Note that both *P. obliquiloculata* and *P. finalis* extend to the present day, although most biologists recognize only *P. obliquiloculata*. Based on Pearson and Penny (2021) as revised by Pearson et al. (2023).

an initially sinistrally dominated population. Both *Neogloboquadrina* and *Pulleniatina* subsequently exhibit the curious pattern of changing their preferred coiling direction through time, although they do so independently of each other (see Discussion in Pearson and Penny, 2021).

A second line of evidence that supports the view that *N. acostaensis* is the ancestor of *Pulleniatina*, as suggested by Banner and Blow (1967) and various subsequent authors, lies in the morphology of the inner juvenile whorl of modern *Pulleniatina obliquiloculata* and *P. finalis*, which supposedly resembles *N. acostaensis*, in a case of ontogeny recapitulating phylogeny. We also found a close similarity between the juvenile form of *N. acostaensis* and the juveniles of most of the *Pulleniatina* morphospecies (Figs. 5 and 6), except that successive chambers in *N. acostaensis* are much smaller. There are many other species in the Cenozoic that have a similar generalized morphology (globanomalinids, parasubbotinids, paragloborotaliids), although none of these existed in the Late Miocene. With the fossil record of planktonic foraminifera as closely sampled as it is, there is no better candidate than *N. acostaensis* among other planktonic foraminifer species existing at that time.

It has been found that *Neogloboquadrina* and *Pulleniatina* are genetically similar, based on their ribosomal DNA (e.g. Darling and Wade, 2008; Aurahs et al., 2009; Morard et al., 2024). In the most recent phylogenetic reconstruction (Morard et al., 2024), *Pulleniatina* forms a clade nested within a paraphyletic *Neogloboquadrina*, with *N. dutertrei* as the closest living relative. This result is as expected if *Pulleniatina* evolved from *N. acostaensis* because palaeontologists have long recognized *N. dutertrei* to be the modern representative morphospecies of the *acostaensis – humerosa – dutertrei* lineage (e.g. Stainforth et al., 1975; Kennett and Srinivasan, 1983; Bolli et al., 1985; Biolzi, 1991). The weight of evidence therefore supports the notion that *Pulleniatina primalis* was an evolutionary offshoot of *Neogloboquadrina acostaensis*, as suggested by Banner and Blow (1967), and that the branching probably occurred after the split between the ancestors of modern *N. dutertrei* and *N. pachyderma*.

Neogloboquadrina acostaensis was a cosmopolitan species, rather generalized in morphology, and crucially it continued for ∼2 million years without any apparent change after the time of the speciation (Raffi et al., 2020). *Pulleniatina primalis* was initially restricted to the tropical Indo-Pacific, probably initially the Pacific (see palaeogeographic maps in Pearson et al., 2023). The speciation event therefore seems to have followed a "budding" pattern and

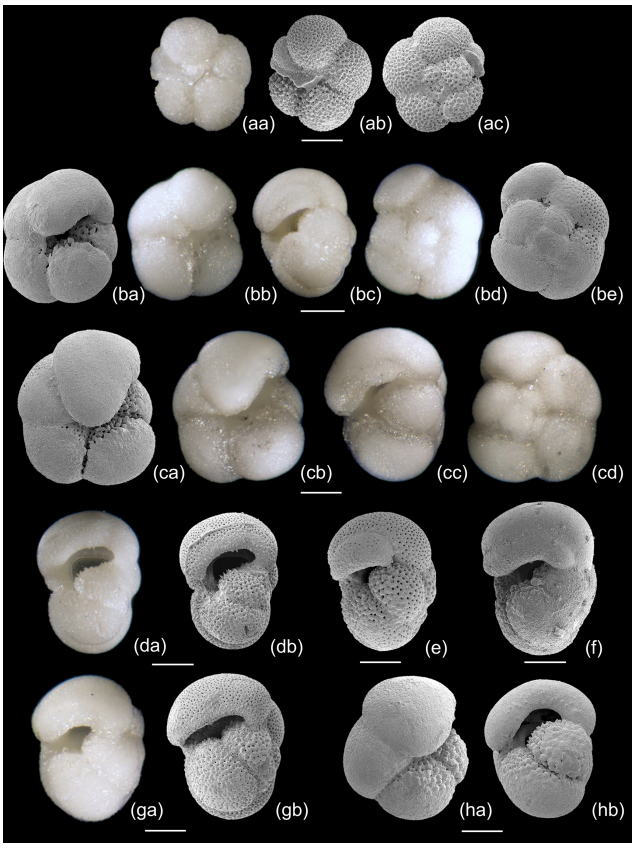

Figure 13. Selected planktonic foraminifera from Sample U1488A-21H-6, 9-11 cm, illustrated to a common scale. **(aa–ac)** *Neogloboquadrina acostaensis*, z-stack LM and SEM. **(ba–hb)** *Pulleniatina primalis*, z-stack LM and SEM. Several of the specimens **(da–b, e, ga–b)** lack a cortex and are probably pregametogenic. The cortex on the others is not fully enveloping, especially in the umbilical area, sutures and patches on the spiral side. Scale bar 100 µm.

was sympatric, i.e. occurring within the geographic range of the ancestor, albeit not across the entire range. The much larger proloculus of *P. primalis*, the divergent ontogeny in the adult stage, and the evolution of a smooth cortex all suggest that founding populations crossed an adaptive threshold of some sort and rapidly evolved away from the ancestral state to exploit a new and ultimately successful ecological niche in which the descendants became abundant and diversified. The fact that the earliest *P. primalis* appear restricted to the tropical Indo-Pacific indicates that the evolutionary transition likely happened there. Modern *Pulleniatina* are relatively deep-dwelling herbivores, suggesting that a new way of life was found within that wider niche. According to Toue et al. (2022), both *Neogloboquadrina dutertrei* and *P. obliquiloculata* share a similar habitat in the modern ocean in subsurface water, occupying separate ecological niches due to a different diet: detritivore in *N. dutertrei* and predominantly herbivore in *P. obliquiloculata*. The evolution of *Pulleniatina* might well be an example of a sub-population exploiting a new food supply and rapidly adapting to a new way of life while leaving the ancestral species essentially unchanged.

4.3.2 The *praespectabilis – spectabilis* lineage

Pulleniatina primalis seems to have gradually diverged into two distinct evolutionary lineages in the Late Miocene (∼ 5.5 Ma), although the split has yet to be studied morphometrically. The *P. praespectabilis – spectabilis* lineage became progressively more angulo-conical through time, and its geographic range, initially restricted to the tropical Indo-Pacific, contracted further into the equatorial Pacific (Pearson et al., 2023). Our data show that both *P. praespectabilis* and *P. spectabilis* had an accelerated growth trajectory relative to other *Pulleniatina*. The transition from a flat-coiling juvenile to a more trochospiral neanic stage occurred slightly earlier in the ontogeny, after Chamber 5 rather than Chamber 6, and the rate of chamber volume increase was significantly "faster" thereafter. The adult stage was reached after about Chamber 10 rather than Chamber 12/13 as in *P. primalis*. If chambers were added daily, the growth may also have been faster in real time. We also note that our specimen of *P. spectabilis* is quite thin-walled in comparison to *P. praespectabilis*, although whether this is typical of populations has yet to be established. The combined evidence points to increasing specialization in this phylogenetic branch, which may also have made the lineage more vulnerable to extinction, which occurred at 4.27 ± 0.05 Ma (Pearson et al., 2023).

4.3.3 The *praecursor – obliquiloculata – finalis* lineage

Pulleniatina primalis appears to have evolved a more generalist mode of life after the divergence with *P. spectabilis*, expanding its geographic range by invading the South China Sea around 5.7 Ma and the Atlantic, mid-latitude North Pacific, and mid-latitude South Pacific around 5.3 Ma (Pearson et al., 2023). It also embarked on a separate evolutionary trajectory involving increasing size, globularity, streptospirality, involution, and wall thickness, which led through the *P. praecursor* morphology towards the modern *P. obliquiloculata* and *P. finalis*. The wall thickness presumably affects the buoyancy of the test (e.g. Duan et al., 2022), and the thick walls of the living species may be related to the deep-dwelling habitat and, with the addition of a dense cortex, to a reproductive strategy involving sinking before reproduction (Schiebel and Hemleben, 2017). The lineage was locally extinct in the Atlantic between 3.27 and 2.24 Ma (Pearson et al., 2023).

Repeated reversals in the preferred coiling direction may point to an evolutionary mode in which a succession of closely related genotypes evolved, coexisted, and occasionally replaced one another, but without leading to lasting morphological divergence (Pearson and Penny, 2021). Modern

populations are extremely diverse in their ribosomal DNA in comparison to other planktonic foraminifera (Morard et al., 2024). The main genotype groups have somewhat contrasting geographic distributions and may be reproductively isolated from one another (Ujiié and Ishitani, 2016). Nevertheless, modern *Pulleniatina* are generally regarded as belonging to a single biological species, and there is no evidence of lasting ecological speciation as we suggest happened earlier with the divergence of the *praespectabilis – spectabilis* lineage. More work needs to be done on the *P. finalis* morphotype to investigate whether the morphological differences with *P. obliquiloculata* that we have observed – principally in proloculus size, streptospirality, and wall thickness – are typical of distinct forms or variable in populations. Marine biologists and geneticists working in the modern age generally do not distinguish *P. finalis* as a morphology, so it is currently unclear how it might map on to the various genotypes that have been identified. However, we note that it has existed across both the tropical Atlantic and the Indo-Pacific since 1.97 ± 0.17 Ma, indicating that it is not a localized or specialized form (Pearson et al., 2023). If it is a megalospheric variant caused by asexual reproduction, it might be typical of the early stages of algal blooms when organisms reproduce rapidly to exploit a patchy resource, with the sexual reproductive phase possibly occurring the waning phases of blooms. This hypothesis needs to be tested by observations of living populations and may also leave a fingerprint in the test geochemistry.

5 Summary and conclusion

We have investigated the morphology of six *Pulleniatina* morphospecies and their putative ancestor, *Neogloboquadrina acostaensis*, using light microscopy, SEM, and micro-CT of representative specimens. Our observations support the view that the various morphospecies are closely related to one another and that the first species, *P. primalis*, most likely evolved from *N. acostaensis*, as has been the general view since Banner and Blow (1967). The evolutionary transition has yet to be fully documented, however. The apertural lip in *N. acostaensis* is an adult feature that does not occur in *Pulleniatina.* We extended the standard bilamellar model of test construction to include the concept of a "modification layer", which, in this instance, wraps around the apertural region in both *N. acostaensis* and *Pulleniatina*, forming a smooth surface and presumably strengthening the area around the aperture. The cortex in *Pulleniatina*, a feature apparently unique to the genus, may have evolved from a local modification layer to extend across the entire test during gametogenesis. *Pulleniatina* split into two evolutionary lineages, one of which (the *praespectabilis – spectabilis* lineage) seems to have evolved a specialist mode of life involving an anguloconical shape and accelerated growth, becoming extinct in the Pliocene. The other more generalist lineage (*praecursor – obliquiloculata – finalis*) seems to have evolved a progressively more involute, streptospiral, and thick-walled morphology that continues to thrive in the modern ocean. The biological status of *P. finalis* (whether it is one morphological extreme of the general population of *P. obliquiloculata*, an asexually produced megalospheric variant, or a distinct biospecies) is currently unresolved.

Data availability. Volumetric and biometric data are available in the Dryad digital repository (https://datadryad.org/, last access: 24 June 2025) at https://doi.org/10.5061/dryad.41ns1rnrd (Fabbrini et al., 2025).

Sample availability. Specimens listed in Table 1 are deposited in the Natural History Museum, London (UK).

All 3D models and tiff stacks of the specimens are available on MorphoSource (https://www.morphosource.org, last access: 24 June 2025): *Neogloboquadrina acostaensis* (https://doi.org/10.17602/M2/M717827, Fabbrini, 2025a), *Pulleniatina primalis* 1 (https://doi.org/10.17602/M2/M717815, Fabbrini, 2025b) *Pulleniatina primalis* 2 (https://doi.org/10.17602/M2/M717993, Fabbrini, 2025c), *Pulleniatina praespectabilis* (https://doi.org/10.17602/M2/M718299, Fabbrini, 2025d), *Pulleniatina spectabilis* (https://doi.org/10.17602/M2/M718446, Fabbrini, 2025e), *Pulleniatina praecursor* (https://doi.org/10.17602/M2/M718749, Fabbrini, 2025f), *Pulleniatina obliquiloculata* (https://doi.org/10.17602/M2/M718604, Fabbrini, 2025g), *Pulleniatina finalis* (https://doi.org/10.17602/M2/M718709, Fabbrini, 2025h).

Supplement. The supplement related to this article is available online at https://doi.org/10.5194/jm-44-213-2025-supplement.

Author contributions. AF and PNP conceptualized the main research question of the study. PNP collected all micropalaeontological data, wrote and curated the article, and created most of the figures. AF segmented and curated the digital volumetric analysis, created some of the figures, and contributed to writing the paper. AB performed the biometric analysis and assisted in writing the paper and creating the figures. THGE corrected and commented on the final draft of the article. BSW corrected the draft and figures and provided analytical facilities and access to samples. All authors discussed the results and commented on the paper.

Competing interests. The contact author has declared that none of the authors has any competing interests.

Disclaimer. Publisher's note: Copernicus Publications remains neutral with regard to jurisdictional claims made in the text, published maps, institutional affiliations, or any other geographical representation in this paper. While Copernicus Publications makes ev-

ery effort to include appropriate place names, the final responsibility lies with the authors.

Acknowledgements. We thank the International Ocean Discovery Program, sponsored by the US National Science Foundation and participating countries, for providing access to samples. The authors are grateful to Jim Davy for assistance with SEM and z-stack light microscope imaging.

Financial support. This research was supported by Natural Environment Research Council grant no. NE/P019013/1 to Bridget S. Wade and grant no. NE/P016375/1 to Paul N. Pearson. Shipboard support was also provided by the Natural Environment Research Council to Bridget S. Wade and Paul N. Pearson (grant no. NE/P016375/1). This work was also supported by the National Research Facility for Lab X-ray CT (NXCT) through EPSRC grant no. EP/T02593X/1, and Thomas H. G. Ezard and Anieke Brombacher were funded by the Natural Environment Research Council (grant no. NE/P019269/1).

Review statement. This paper was edited by Sev Kender and reviewed by Adriane Lam and Tracy Aze.

References

Aurahs, R., Göker, M., Grimm, G. W., Hemleben, V., Hemleben, C., Schiebel, R., and Kučera, M.: Using the multiple analysis approach to reconstruct phylogenetic relationships among planktonic Foraminifera from highly divergent and length-polymorphic SSU rDNA sequences, Bioinformatics and Biology Insights, 3, BBI-S3334, https://doi.org/10.4137/BBI.S3334, 2009.

Banner, F. T. and Blow, W. H.: The origin, evolution and taxonomy of the foraminiferal genus *Pulleniatina* Cushman, 1927, Micropaleontology, 13, 133–162, 1967.

Bé, A. W. H.: Gametogenic calcification in a spinose planktonic foraminifer, *Globigerinoides sacculifer* (Brady), Mar. Micropaleontol., 5, 283–310, 1980.

Bé, A. W. H., Hemleben, C., Anderson, O. R., and Spindler, M.: Pore structures in planktonic foraminifera, J. Foramin. Res., 10, 117–128, https://doi.org/10.2113/gsjfr.10.2.117, 1980.

Belyea, P. R. and Thunell, R. C.: Fourier shape analysis and planktonic foraminiferal evolution: the *Neogloboquadrina-Pulleniatina* lineages, J. Paleontol., 58, 1026–1040, 1984.

Berger, W. H. and Soutar, A.: Planktonic foraminifera: field experiment on production rate, Science, 156, 1495–1497, 1967.

Biolzi, M.: Morphometric analyses of the Late Neogene planktonic foraminiferal lineage *Neogloboquadrina dutertrei*, Mar. Micropaleontol., 18, 129–142, 1991.

Bolli, H. M., Loeblich, A. R., and Tappan, H.: Planktonic foraminiferal families Hantkeninidae, Orbulinidae, Globorotaliidae and Globotruncanidae, in: Studies in Foraminifera, edited by: Loeblich, A. R., Tappan, H., Beckmann, J. P., Bolli, H. M., Montanaro Gallitelli, E., and Troelsen, J. C., United States National Museum Bulletin 215, 3–50, 1957.

Bolli, H. M., Saunders, J. B., and Perch-Nielsen, K. (Eds.): Plankton stratigraphy: volume 1, Planktic Foraminifera, Calcareous Nannofossils and Calpionellids, Cambridge University Press, Cambridge, ISBN 0 521 23576 6, 1985.

Brady, H. B.: Report on the foraminifera dredged by HMS Challenger, during the years 1873–1876, Report of Scientific Results of the Exploration Voyage of HMS Challenger, Zoology, 9, 1–814, 1884.

Brombacher, A., Searle-Barnes, A., Zhang, W., and Ezard, T. H. G.: Analysing planktonic foraminiferal growth in three dimensions with foram3D: an R package for automated trait measurements from CT scans, J. Micropalaeontol., 41, 149–164, https://doi.org/10.5194/jm-41-149-2022, 2022.

Brönnimann, P. and Resig, J.: A Neogene globigerinacean biochronologic time-scale of the southwestern Pacific, Initial Rep. Deep Sea, 7, 1235–1469, https://doi.org/10.2973/dsdp.proc.7.128.1971, 1971.

Brummer, G. J. A. and Kroon, D.: Planktonic foraminifers as tracers of ocean-climate history: Ontogeny, relationships and preservation of modern species and stable isotopes, phenotypes and assemblage distribution in different water masses, Free University Press, ISBN 9789062567447, 1988.

Brummer, G.-J. A. and Kučera, M.: Taxonomic review of living planktonic foraminifera, J. Micropalaeontol., 41, 29–74, https://doi.org/10.5194/jm-41-29-2022, 2022.

Brummer, G. J. A., Hemleben, C., and Spindler, M.: Ontogeny of extant spinose planktonic foraminifera (Globigerinidae): A concept exemplified by *Globigerinoides sacculifer* (Brady) and *G. ruber* (d'Orbigny), Mar. Micropaleontol., 12, 357–381, 1987.

Burke, J. E., Renema, W., Schiebel, R., and Hull, P. M.: Three-dimensional analysis of inter-and intraspecific variation in ontogenetic growth trajectories of planktonic foraminifera, Mar. Micropaleontol., 155, 101794, https://doi.org/10.1016/j.marmicro.2019.101794, 2020.

Burt, B. J. and Scott, G. H.: Spinosity and coiling geometry in *Pulleniatina* (foraminifera), J. Foramin. Res., 5, 166–175, 1975.

Chen, W. L., Kang, J. C., Kimoto, K., Song, Y. F., Yin, G. C., Swisher, R. E., Lu, C. H., Kuo, L. W., Huang, J. J., and Lo, L.: μ-Computed tomographic data of fossil planktonic foraminifera from the western Pacific Ocean: a dataset concerning two biostratigraphic events during the Early Pleistocene, Frontiers in Ecology and Evolution, 25, 1171891, https://doi.org/10.3389/fevo.2023.1171891, 2023.

Coletti, G., Stainbank, S., Fabbrini, A., Spezzaferri, S., Foubert, A., Kroon, D., and Betzler, C.: Biostratigraphy of large benthic foraminifera from Hole U1468A (Maldives): a CT-scan taxonomic approach, Swiss J. Geosci., 111, 523–536, https://doi.org/10.1007/s00015-018-0306-7, 2018.

Cushman, J. A.: An outline of a reclassification of the Foraminifera, Contributions from the Cushman Laboratory for Foraminiferal Research, 3, 1–105, 1927.

Darling, K. F. and Wade, C. M.: The genetic diversity of planktic foraminifera and the global distribution of ribosomal RNA genotypes, Mar. Micropaleontol., 67, 216–238, https://doi.org/10.1016/j.marmicro.2008.01.009, 2008.

Darling, K. F., Husum, K., and Fenton, I. S.: The biphasic life cycle of the non-spinose planktonic foraminifera is characterised by an aberrant coiling signature, Mar. Micropaleontol., 185, 102295, https://doi.org/10.1016/j.marmicro.2023.102295, 2023.

Duan, B., Li, T., and Pearson, P. N.: Three dimensional analysis of ontogenetic variation in fossil globorotaliiform planktic foraminiferal tests and its implications for ecology, life processes and functional morphology, Mar. Micropaleontol., 165, 101989, https://doi.org/10.1016/j.marmicro.2021.101989, 2021.

Duan, B., Tiegang L., and Pearson, P. N.: Three dimensional analysis of ontogenetic variation in fossil globorotaliiform planktic foraminiferal tests and its implications for ecology, life processes and functional morphology, Mar. Micropaleontol., 165, 101989, https://doi.org/10.1016/j.marmicro.2021.101989, 2021.

Fabbrini, A.: Media 000717827: *Neogloboquadrina acostaensis*, MorphoSource [sample], https://doi.org/10.17602/M2/M717827, 2025a.

Fabbrini, A.: Media 000717815: *Pulleniatina primalis*, MorphoSource [sample], https://doi.org/10.17602/M2/M717815, 2025b.

Fabbrini, A.: Media 000717993: *Pulleniatina primalis*, MorphoSource [sample], https://doi.org/10.17602/M2/M717993, 2025c.

Fabbrini, A.: Media 000718299: *Pulleniatina praespectabilis*, MorphoSource [sample], https://doi.org/10.17602/M2/M718299, 2025d.

Fabbrini, A.: Media 000718446: *Pulleniatina spectabilis*, MorphoSource [sample], https://doi.org/10.17602/M2/M718446, 2025e.

Fabbrini, A.: Media 000718749: *Pulleniatina praecursor*, MorphoSource [sample], https://doi.org/10.17602/M2/M718749, 2025f.

Fabbrini, A.: Media 000718604: *Pulleniatina obliquiloculata*, MorphoSource [sample], https://doi.org/10.17602/M2/M718604, 2025g.

Fabbrini, A.: Media 000718709: *Pulleniatina finalis*, MorphoSource [sample], https://doi.org/10.17602/M2/M718709, 2025h.

Fabbrini, A., Greco, M., Iacoviello, F., Kucera, M., Ezard, T. H., and Wade, B. S.: Bridging the extant and fossil record of planktonic foraminifera: implications for the *Globigerina* lineage, Palaeontology, 66, e12676, https://doi.org/10.1111/pala.12676, 2023.

Fabbrini, A., Pearson, P., Brombacher, A., Iacoviello, F., Ezard, T., and Wade, B.: Morphology of Pulleniatina (*planktonic foraminifera*): Micro-CT internal volumes, Dryad [data set], https://doi.org/10.5061/dryad.41ns1rnrd, 2025.

Fehrenbacher, J. S., Russell, A. D., Davis, C. V., Gagnon, A. C., Spero, H. J., Cliff, J. B., Zhu, Z., and Martin, P.: Link between light-triggered Mg-banding and chamber formation in the planktic foraminifera *Neogloboquadrina dutertrei*, Nat. Comm., 8, 15441, https://doi.org/10.1038/ncomms15441, 2017.

Görög, Á., Szinger, B., Tóth, E., and Viszkok, J.: Methodology of the micro-computer tomography on foraminifera, Palaeontol. Electron., 15, 3T, https://doi.org/10.26879/261, 2012.

Hemleben, C., Spindler, M., and Anderson, O. R.: Modern Planktonic Foraminifera, Springer, New York, 363 pp., ISBN 978-1-4612-8150-4, 1989.

Iwasaki, S., Kimoto, K., Okazaki, Y., and Ikehara, M.: Micro-CT scanning of tests of three planktic foraminiferal species to clarify dissolution process and progress, Geochem. Geophys. Geosy., 20, 6051–6065, https://doi.org/10.1029/2019GC008456, 2019.

Jonkers, L., Reynolds, C. E., Richey, J., and Hall, I. R.: Lunar periodicity in the shell flux of planktonic foraminifera in the Gulf of Mexico, Biogeosciences, 12, 3061–3070, https://doi.org/10.5194/bg-12-3061-2015, 2015.

Kennett, J. P. and Srinivasan, M. S.: Neogene Planktonic Foraminifera, a Phylogenetic Atlas, Hutchinson Ross, Stroudsberg, Pennsylvania, 265 pp., ISBN 978-0879330705, 1983.

Kimoto, K. and Tsuchiya, M.: The "unusual" reproduction of planktonic foraminifera: an asexual reproductive phase of *Neogloboquadrina pachyderma* (Ehrenberg), Anuario do Instituto de Geociencias, Universidade Federal do Rio de Janeiro, 29, p. 461, https://doi.org/10.11137/2006_1_461-461, 2006.

Kunioka, D., Shirai, K., Takahata, N., Sano, Y., Toyofuku, T., and Ujiie, Y.: Microdistribution of Mg/Ca, Sr/Ca, and Ba/Ca ratios in Pulleniatina obliquiloculata test by using NanoSIMS: implication for the vital effect mechanism, Geochem. Geophys. Geosy., 7, 11, https://doi.org/10.1029/2006GC001280, 2006.

Lastam, J., Griesshaber, E., Yin, X., Rupp, U., Sánchez-Almazo, I., Hess, M., Walther, P., Checa, A., and Schmahl, W. W.: Patterns of crystal organization and calcite twin formation in planktonic, rotaliid, foraminifera shells and spines, J. Struct. Biol., 215, 107898, https://doi.org/10.1016/j.jsb.2022.107898, 2023a.

Lastam, J., Griesshaber, E., Yin, X., Rupp, U., Sánchez-Almazo, I., Heß, M., Walther, P., Checa, A., and Schmahl, W. W.: The unique fibrillar to platy nano-and microstructure of twinned rotaliid foraminiferal shell calcite, Sci. Rep., 13, 2189, https://doi.org/10.1038/s41598-022-25082-9, 2023b.

Leckie, R. M., Wade, B. S., Pearson, P. N., Fraass, A. J., King, D. J., Olsson, R. K., Silva, I. P., Spezzaferri, S., and Berggren, W. A.: Taxonomy, biostratigraphy, and phylogeny of Oligocene and early Miocene *Paragloborotalia* and *Parasubbotina*, in: Cushman Foundation of Foraminiferal Research, Atlas of Oligocene Planktonic Foraminifera, edited by: Wade, B. S., Olsson, R. K., Pearson, P. N., Huber, B. T., and Berggren, W. A., Special Publication, No. 46, 125–178, ISBN 9781970168419, 2018.

Meilland, J., Ezat, M. M., Westgård, A., Manno, C., Morard, R., Siccha, M., and Kucera, M.: Rare but persistent asexual reproduction explains the success of planktonic foraminifera in polar oceans, J. Plankton Res., 45, 15–32, https://doi.org/10.1093/plankt/fbac069, 2023.

Morard, R., Darling, K. F., Weiner, A. K., Hassenrück, C., Vanni, C., Cordier, T., Henry, N., Greco, M., Vollmar, N. M., Milivojevic, T., and Rahman, S. N.: The global genetic diversity of planktonic foraminifera reveals the structure of cryptic speciation in plankton, Biol. Rev., 99, 1218–1241, https://doi.org/10.1111/brv.13065, 2024.

Parker, F. L.: A new planktonic species (Foraminiferida) from the Pliocene of Pacific Deep-Sea cores, Contributions from the Cushman Foundation for Foraminiferal Research, 16, 151–153, 1965.

Parker, W. K. and Jones, T. R.: On some Foraminifera from the North Atlantic and Arctic Oceans, including Davis Straits and Baffin's Bay, Philos. T. R. Soc. Lond., 155, 325–441, 1865.

Pearson, P. N. and Penny, L.: Coiling directions in the planktonic foraminifer *Pulleniatina*: A complex eco-evolutionary dynamic spanning millions of years, PloS one, 16, e0249113, https://doi.org/10.1371/journal.pone.0249113, 2021.

Pearson, P. N., John, E., Wade, B. S., D'haenens, S., and Lear, C. H.: Spine-like structures in Paleogene muricate planktonic foraminifera, J. Micropalaeontol., 41, 107–127, 2022.

Pearson, P. N., Young, J., King, D. J., and Wade, B. S.: Biochronology and evolution of *Pulleniatina* (planktonic foraminifera), J. Micropalaeontol., 42, 211–255, https://doi.org/10.5194/jm-42-211-2023, 2023.

Pearson, P. N., Fabbrini, A., and Wade, B. S.: Systematic taxonomy of *Pulleniatina*, J. Foramin. Res., 55, 245–275, https://doi.org/10.61551/gsjfr.55.3.245, 2025.

Postuma, J. A.: Manual of Planktonic Foraminifera, Elsevier, New York, 420 pp., 1971.

Procter, F. A., Piazolo, S., John, E. H., Walshaw, R., Pearson, P. N., Lear, C. H., and Aze, T.: Electron backscatter diffraction analysis unveils foraminiferal calcite microstructure and processes of diagenetic alteration, Biogeosciences, 21, 1213–1233, https://doi.org/10.5194/bg-21-1213-2024, 2024.

Raffi, I., Wade, B. S., and Pälike, H.: The Neogene Period, edited by: Gradstein, F. M., Ogg, J. G., Schmitz, M. D., and Ogg, G.M., in: Geologic Time Scale 2020, 1141–1215, https://doi.org/10.1016/B978-0-12-824360-2.00029-2, 2020.

Reiss, Z.: The Bilamellidea, nov. superfam. and remarks on Cretaceous globorotaliids, Contrib. Cushman Found. Foram. Res., 8, 127–145, 1957.

Reiss, Z. and Hottinger, L.: The Gulf of Aqaba: Ecological Micropaleontology, Vol. 50, Springer Science & Business Media, 19–32, https://doi.org/10.1007/978-3-642-69787-6, 1984.

Rosenthal, Y., Holbourn, A. E., Kulhanek, D. K., Aiello, I. W., Babila, T. L., Bayon, G., Beaufort, L., Bova, S. C., Chun, J.-H., Dang, H., Drury, A. J., Dunkley Jones, T., Eichler, P. P. B., Fernando, A. G. S., Gibson, K., Hatfield, R. G., Johnson, D. L., Kumagai, Y., Li, T., Linsley, B. K., Meinicke, N., Mountain, G. S., Opdyke, B. N., Pearson, P. N., Poole, C. R., Ravelo, A. C., Sagawa, T., Schmitt, A., Wurtzel, J. B., Xu, J., Yamamoto, M., and Zhang, Y. G.: Site U1488, in: Western Pacific Warm Pool, edited by: Rosenthal, Y., Holbourn, A. E., and Kulhanek, D. K., Proceedings of the International Ocean Discovery Program, 363, https://doi.org/10.14379/iodp.proc.363.109.2018, 2018.

Schiebel, R. and Hemleben, C.: Planktic foraminifers in the Modern Ocean, Berlin, Springer, 358 pp., ISBN 978-3-662-50297-6, 2017.

Schiebel, R., Bijma, J., and Hemleben, C.: Population dynamics of the planktic foraminifer *Globigerina bulloides* from the eastern North Atlantic, Deep-Sea Res. Pt. I,, 44, 1701–1713, 1997.

Spindler, M., Hemleben, C., Bayer, U., Bé, A. W. H., and Anderson, O. R.: Lunar periodicity of reproduction in the planktonic foraminifer *Hastigerina pelagica*, Mar. Ecol. Prog. Ser., 1, 61–64, 1979.

Stainforth, R. M., Lamb, J. L., Luterbacher, H., Beard, J. H., and Jeffords, R. M.: Cenozoic Planktonic Foraminiferal Zonation and Characteristics of Index Forms, The University of Kansas Paleontological Contributions, 62, 425 pp., 1975.

Steinhardt, J., de Nooijer, L. L., Brummer, G. J., and Reichart, G. J.: Profiling planktonic foraminiferal crust formation, Geochem. Geophy. Geosy., 16, 2409–2430, 2015.

Subbotina, N. N., Voloshinova, N. A., and Azbel, A. J.: Vvedenie v izuchenie foraminifer (Klassifikaciya melkich foraminifer Mezo-Kaynozoya) [Introduction to the foraminiferal study (Classification of the small Meso-Cenozoic foraminifera)], Leningrad, Nedra, Leningradskoe otdelenie, 212 pp., 1981 (in Russian).

Sverdlove, M. S. and Bé, A. W.: Taxonomic and ecological significance of embryonic and juvenile planktonic foraminifera, J. Foramin. Res., 15, 235–251, https://doi.org/10.2113/gsjfr.15.4.235, 1985.

Takagi, H., Kurasawa, A., and Kimoto, K.: Observation of asexual reproduction with symbiont transmission in planktonic foraminifera, J. Plankton Res., 42, 403–410, https://doi.org/10.1093/plankt/fbaa033, 2020.

Toue, R., Fujita, K., Tsuchiya, M., Chikaraishi, Y., Sasaki, Y., and Ohkouchi, N.: Trophic niche separation of two non-spinose planktonic foraminifers *Neogloboquadrina dutertrei* and *Pulleniatina obliquiloculata*, Prog. Earth Planet. Sc., 9, 1–11, https://doi.org/10.1186/s40645-022-00478-3, 2022.

Ujiié, Y. and Ishitani, Y.: Evolution of a planktonic foraminifer during environmental changes in the tropical oceans, PLoS One, 11, e0148847, https://doi.org/10.1371/journal.pone.0148847, 2016.